

Degeneration of cholinergic basal forebrain nuclei after focally evoked status epilepticus

Francesca Biagioni¹, Anderson Gaglione¹, Filippo S. Giorgi^{2,3}, Domenico Bucci¹, Slavianka Mojanova¹, Antonio De Fusco^{1,a}, Michele Madonna¹, Francesco Fornai^{1,2}

¹I.R.C.C.S. Neuromed, via dell'Electronica 4, 86077, Pozzilli (IS), Italy

²Department of Translational Research and New Technologies in Medicine and Surgery, University of Pisa, via Roma 55, 56126, Pisa, Italy

³Section of Neurology, Pisa University Hospital, Department of Clinical and Experimental Medicine, University of Pisa, via Roma 67, 56126, Pisa, Italy

^aPresent address of Antonio De Fusco: Center for Synaptic Neuroscience and Technology, Istituto Italiano di Tecnologia, Department of Experimental Medicine, University of Genova, Genova, Italy.

Corresponding Author

Prof. Francesco Fornai = Francesco.fornai@neuromed.it; francesco.fornai@med.unipi.it

Abstract

Status epilepticus (SE) of limbic onset might cause degenerative phenomena in different brain structures, and may be associated with chronic cognitive and EEG effects. In the present study SE was evoked focally in rats by microinfusing picomolar doses of cyclothiazide+bicuculline into the anterior extent of the piriform cortex (APC), the so-called *area tempestas*, an approach which allows to evaluate selectively the effects of seizure spreading through the natural anatomical circuitries, up to secondary generalization. In the brains of rats submitted to SE we analyzed neuronal density, occurrence of degenerative phenomena (by Fluoro-Jade B -FJB- staining) and expression of heat shock protein-70 (HSP-70) in the piriform cortex and hippocampus, and FJB-staining in ventromedial thalamus. We further analysed in detail, the loss of cholinergic neurons, and the presence of FJB- and HSP-70 positive neurons in basal forebrain cholinergic areas, i.e. the medial septal nucleus (MSN, Ch1), the diagonal band of Broca (DBB, Ch2 and Ch3) and the Nucleus basalis of Meynert (NBM, Ch4). In fact, these nuclei are strictly connected with limbic structures, and play a key pivotal role in different cognitive functions and vigilance. Although recent studies begun to investigate these nuclei in experimental epilepsy and in epileptic patients, conflicting results were obtained so far. We showed that after long-lasting, focally induced SE there is a significant cell loss within all of the abovementioned cholinergic nuclei ipsi- and contralaterally to the infusion site. In parallel, these nuclei show also FJB-positive neurons and heat shock protein-70 expression. We also showed the occurrence of cell loss and/or degenerative phenomena in limbic cortex, hippocampus and limbic thalamic areas. Those effects vary depending on the single nucleus assessed and on the severity of the SE seizure score (as rats were further divided in a low- and a high severity behavioural seizure score group). These novel findings show direct evidence of SE-induced neuronal damage which is solely due to seizure activity ruling out potential confounding effects produced by systemic pro-convulsant neurotoxins. A damage to basal forebrain cholinergic nuclei which may underlie cognitive alterations is documented for the first time in a model of SE triggered focally.

Keywords: status epilepticus; anterior piriform cortex; Area Tempestas; cholinergic nuclei; septal nucleus; nucleus basalis of Meynert; diagonal band of Broca; electroencephalogram; fluoro-jade B; heat shock protein-70.

1. Introduction

Temporal lobe seizures are by far the most common types of seizures in humans (Panayiotopoulos, 2002), and they originate in the mesial temporal lobe structures, which in most cases correspond to allo- or meso-cortical limbic areas. Often seizures remain limited within limbic structures while, sometimes, they may become generalized. By definition, seizures are self-limiting, lasting less than 2-3 min. However, when self-limiting mechanisms fail, seizures can prolong as continuous convulsive activity lasting over **5 min**, which characterizes a seizure activity defined as "status epilepticus" (SE)(**for more detailed definitions of subtypes of SE, see also Trinka et al., 2015**) .

A major question related to SE is whether SE of focal origin can cause detrimental effects to the brain, and if this occurs, which is the severity and site-specificity of these effects. These questions cannot be fully answered in humans, as in the routine clinical *scenario* one can evaluate SE patients only after they have experienced prolonged SE (whose precise duration can be rarely assessed), and imaging data are obtained only after SE and cannot be compared with pre-seizure ones.

In the past decades several models of limbic SE have been developed in rodents: the most widely used consist in systemic administration of kainic acid (KA, an AMPA/KA glutamic acid receptor agonist) and pilocarpine (a muscarinic cholinergic receptor agonist) (for reviews, see Turski et al., 1983; Tremblay et al., 1984; Nitecka et al., 1984). In these models, animals show prolonged limbic seizures, which may evolve into secondarily generalized ones, and SE which can last up to several hours. SE induced by these approaches causes cell loss in different brain regions, including the hippocampus thalamus and neocortex (e.g. see Nitecka et al., 1984). **In patients, SE of limbic origin potentially can spread to other limbic or extra-limbic areas through the natural anatomical pathways reciprocally connected with the triggering site. Thus, animal models in which SE is induced focally in the limbic system might be closer to the human condition compared with systemic KA or pilocarpine. In particular, this might allow to decipher what is really produced by the engagement of neurons during seizure and to rule out the potential direct neurotoxic effects of systemically administered kainic acid (Lau et al., 2010) or the**

potential haemodynamic alterations caused by systemic pilocarpine (Dage, 1979). In the last decades different models of focally-induced seizures/SE were produced, including focal electrical stimulation protocols (Lothman et al., 1989) or focal chemoconvulsant infusions, such as intrahippocampal (Schwartz et al., 1978) or intraamygdaloid infusion of Kainic acid (Ben-Ari et al., 1979), or intrahippocampal pilocarpine (Furtado et al., 2002; 2011). In the present study, seizures were evoked focally, from the anterior extent of the deep piriform cortex (APC). This limbic allo-cortical region was shown to possess a very low threshold to induce seizures when focally microinfused with bicuculline, a GABA-A receptor antagonist (Piredda and Gale, 1985). When bicuculline is injected immediately after cyclothiazide (a desensitization blocker of AMPA glutamatergic receptor) into the this region, it induces SE rather than episodic seizures. This SE is self-sustaining and often lasts several hours (Fornai et al., 2000; 2005; Giorgi et al., 2003, 2006, 2008). SE elicited by this approach in most cases is self-sustaining but also self-limited (Fornai et al., 2000; 2005; Giorgi et al. 2003).

This model has proven to be particularly useful to detect which brain areas are selectively engaged by seizures triggered in the APC. This has been assessed by different *in situ* techniques: (i) 2-desoxyglucose uptake (Cassidy and Gale 1998; Dybdal and Gale, 2000; Giorgi et al., 2008); (ii) immediate early gene expression (Maggio et al., 1993; Lanaud et al., 1993; Giorgi et al., 2008); (iii) heat shock protein expression (Shimosaka and Simon, 1992); (iv) focal pharmacological modulation of seizures within selective brain regions supposed to be involved in seizure circuitry (Maggio and Gale, 1989; Shimosaka and Simon, 1994; Halonen et al., 1994; Tortorella et al., 1997; Vismar et al., 2015). Such a model was also demonstrated to own a heuristic value for describing the functional anatomy of limbic circuitries. In fact, a functional mapping of anatomical connectivity and the strength of these connections was recently postulated based on these data (Vismar et al., 2015). Thus, the APC, named *area tempestas* by Dr. Gale when she first described its seizure initiating propensity (Piredda and Gale, 1985), provided a tool to explore brain connectivity beyond seizure activity.

Within this frame we were particularly interested to investigate a group of cholinergic neurons in the basal forebrain which are highly connected with limbic structures and play an important role in different brain functions. These cholinergic nuclei of the basal forebrain are classified as Ch1-4 areas (according to Mesulam et al., 1983a), corresponding to the medial septal nucleus (Ch1) (MSN), the Diagonal Band of Broca (Ch2-Ch3) (DBB), and the Nucleus basalis of Meynert (Ch4) (NBM). They play a pivotal role in learning and memory (e.g. Everitt and Robbins, 1997; Sarter and Bruno, 1997; Roland et al., 2014), apart from playing an activating effect on EEG (e.g., see Buszaki et al., 1988; Furman et al., 2015) and a significant role also in regulating vigilance and sleep/waking state (Szymusiak, 1995; Zant et al., 2016; Lagos et al., 2012), which can also indirectly affect cognition. Patients with seizures originating in limbic structures show often subtle cognitive and sleep alterations, which are not fully explained by the occurrence of hippocampal sclerosis (for a review, see Bell et al., 2011). Even more, SE in patients has been associated by several authors with delayed cognitive impairment (e.g. Dodrill and Wilensky, 1990; see also the review by Helmstaedter, 2007) and this seems to be the case especially after generalized convulsive SE (e.g. Power et al., 2018). Less is known about chronic effects on EEG and sleep parameters by SE (Bazil and Anderson 2001). Similarly to what above mentioned concerning neuronal damage, also the effects of SE on parameters potentially linked with cholinergic functions (cognitive and EEG/sleep), are difficult to assess in patients, mainly because of the potential bias of an effect of the SE- precipitating insult by itself on these parameters, and of the lack of precise knowledge of these parameters in the single patients before SE (e.g. see Helmstaedter, 2007).

Thus, in the present study we wish to disclose whether SE focally induced from APC, apart from altering limbic allocortical and allothalamic regions, may affect NBM, MSN and DBB.

As said, all these cholinergic regions are highly connected with the cerebral cortex and especially with limbic areas. In particular, Ch4 receives direct cortical afferents mainly from the piriform cortex, the medial temporal cortex and entorhinal cortex, orbitofrontal cortex and insula (Mesulam

and Mufson, 1984). Ch1 receives the main cortical afferents from the hippocampus (Haghdoost-Yazdi et al., 2009), but also from the piriform cortex and, to a lesser extent, from the amygdala (Swanson and Cowan, 1979). Ch2 and Ch3 share some afferents from the same areas innervating Ch1 (e.g. hippocampus) (Haghdoost-Yazdi et al., 2009) and are interconnected with Ch1 (Swanson and Cowan, 1979). **Ch1-4 nuclei widely innervate limbic structures, and especially the hippocampus (Mesulam et al., 1983a;b; Zaborszky et al., 2012).**

We show that all three cholinergic nuclei, although with slight differences, show degenerative phenomena after SE induced focally from the APC; we also describe degenerative phenomena in limbic and thalamic structures.

2. Material and Methods

2.1 Animals

50 adult male Sprague-Dawley rats (Harlan Laboratories produced in house) weighing 280-320 g were used. All animals were kept under environmentally controlled conditions (room temperature 22°C; humidity 40%) with food and water *ad libitum* and with a **regular** 12 h light/dark cycle. Rats were handled in accordance with the Guidelines for Animal Care and Use of the National Institutes of Health, and adequate measures were taken to minimize animal pain. (Authorization N° 1204/2015-PR).

2.2 Experimental design and Drugs administration

Rats were submitted to surgery and implanted with a guide cannula into the left APC under deep anaesthesia. Twenty-four h after recovery from surgery they were submitted to microinfusions of either saline or bicuculline+cyclothiazide into the APC and evaluated behaviorally for seizures occurrence. Cyclothiazide (Hellobio, Bristol, UK), was dissolved in a solution of saline + Dimethylsulfoxide (DMSO 20%) (200 pmol in 120 nL); bicuculline methiodide (Sigma Aldrich, Milan, Italy) was dissolved in saline (118 pmol in 120 nL). For cyclothiazide+bicuculline co-

infusions, **120 nL** of cyclothiazide solution and 120 nL of bicuculline solutions were injected into the APC, 5 min apart, at the rate of 60 nL/min. **Control animals were injected with a vehicle solution (saline alone and saline + DMSO 20%), same volumes and flow rates as above, i.e. two infusions of 120nL at 60nL/min, 5 min apart.** Five days after infusions animals were sacrificed and their brains were processed for morphological analysis.

Sub-groups of rats, during the same surgical procedure, were also implanted with EEG electrodes to monitor EEG in baseline conditions and during seizures; these rats were used for EEG recordings only.

2.3 Surgical procedures

Animals were deeply anesthetized with ketamine 60 mg/kg and xylazine 12 mg/kg i.m. and placed in a stereotaxic apparatus (World Precision Instruments, Inc) with the incisor bar set 5 mm above the interaural line. Body temperature was maintained at 37°C by using a rectal thermostat pad instrument. Local anesthesia with Lidocain 2% was applied into the lateral muscles of the head before skin incision. Stereotaxic coordinates for the tip of the internal cannula (see below), corresponding to the APC (Piredda and Gale, 1985), were as follows: AP=+4 mm from the bregma, ML=+3.3 mm from the midline, DV=-6.5 mm below the dura (according to the atlas of Pellegrino et al., 1979). A microinfusion cannula system was prepared before the surgery and used for APC microinfusions. The system consisted of a guide cannula (prepared from a 22-gauge stainless-steel needle -Braun Melungen AG Sterican^R), an injection cannula (prepared from a 27-gauge stainless – steel needle, Braun Malungen AG Sterican^R) connected with PE 20 polyethylene tubing to an infusion pump, and a dummy cannula (same diameter as the injection cannula). For each animal a guide cannula was inserted through a hole drilled in the skull, and secured with acrylic cement and screws. The tip of the guide cannula was placed **1 mm** above the APC and the injection cannula was designed to protrude 1 mm beyond the tip of the guide cannula.

After the surgery, the animals were kept one per cage.

2.4 Focal infusions and seizure evaluation

For drug microinfusions, the internal cannula was inserted into the guide cannula in freely moving animal. Each drug solution/vehicle was injected through the injection cannula, connected via polyethylene tubing to a 10 μ L Hamilton syringe driven by infusion pump (KD Scientific Syringe Pump Co.). After the end of each infusion, the internal cannula was left in place for 1 min for complete solution delivery. Correct cannula placement was verified after sacrifice in Nissl-stained sections (see below): only rats in which the cannula was placed in the APC were used for data analysis.

Animals were observed during 6 hours after the end of microinjection. Seizure severity was evaluated according to the following behavioral score modified from Racine (1972) (see also Fornai et al., 2005; Giorgi et al., 2003; 2008): 0.5=jaw clonus; 1=myoclonic jerks of contralateral forelimb; 2=mild bilateral forelimb clonus lasting 5-15 s; 3=bilateral forelimb clonus lasting more than 15 s; 4=rearing, with concomitant bilateral forelimb clonus; 5=rearing with loss of balance and concomitant forelimb +/- hind limb clonus. It was recorded also the onset of SE, which is defined here as convulsive seizure activity lasting, without any interruption, for at least 5 min'. For each rat we measured seizure duration (time interval between the first and the last ictal event), and the predominant seizure score observed during 5 min' observation time intervals throughout the whole observation period; a seizure score average for the whole seizing period was thus calculated for each animal. Animals were further divided in 2 groups based on seizure severity score: a group with average seizure severity ranging between 1-2 ("low severity" score), and a group showing an average seizure severity ranging between 3-4 ("high severity" score). **Seizures score and features were consistently assessed by a single observer who is trained in assessing behavioral seizures in rats and who was blinded to the treatment.**

2.5 EEG electrodes implantation and recording

For EEG recordings, four animals were implanted with EEG electrodes in the same surgical step of the guide cannula placement.

Electrosubcorticogram (ESCoG) was recorded by cortical wire electrodes [PFA-coated stainless steel wires with diameter of 127.0 (bare)/203.2 (coated) microns, A-M Systems, WA] implanted around the border of cortical layers V and VI (1.5–2.5 mm below the skull surface). **The ESCoG will be referred for simplicity as electroencephalogram (EEG) throughout the remaining text.**

The wire electrodes were inserted through small holes in the skull at the level of the left (ipsilaterally to the infusion of bicuculline) and right primary somatosensory cortex, trunk region (S1Tr) and left frontal motor cortex (M1). The coordinates were as follows: for the S1Tr cortex, AP = -3.6 from bregma, ML = ± 3.0 from midline, and for the ipsilateral M1 cortex, AP = +1.7 from bregma, ML = +2.5 from midline (atlas of Paxinos and Watson, 1997).

Two stainless steel screws (0,80x3,32, Plastics One) served as reference and ground electrodes and were fixed above frontal sinus and cerebellum, respectively. Another screw was inserted into the bone behind the implanted cannula to fix the cannula together with all wires, screws and the attached 6-pin connector with Glass ionomer cement (KetacTM Cem radiopaque).

One week after the surgery each animal was placed into a transparent booth equipped with video camera and a flexible cable connected to a rotating commutator allowing free movement of the animal. The booth was inside of an electrically shielded, light-, sound-, and temperature-controlled video-EEG room. Before each recording, the animal was habituated for 3-5 hours to the environment and then, for another 2 hours, to the tethering system of the recording system.

The monopolar signals (against the reference electrode) were amplified, band passed-filtered between 0.1 and 70 Hz, notch 50 Hz-filtered (if necessary), digitized at 400 Hz, and stored in a computer drive. The recording was made by means of Grass-Technologies 800Hz amplifier, Twin EEG recording system and Grass-Telefactor software (Astro-Med, Inc., W. Warwick, RI, U.S.A.).

A video stream of animal behaviour was simultaneously recorded and stored. Then, a video protocol was created off-line for the time course of the behavioural states with special attention to monitoring and designation of the Racine scores of the bicuculline-induced seizures. The EEG signals were exported as European Data Format (edf) files and analyzed using Acknowledge 4.1.1 software (Biopac Systems, San Francisco, CA, USA). Following linear de-trending and removing

the mean of the signal, a power spectral density (PSD) analysis of the resulting data samples were performed by using Welch approximation algorithm to average signal time-sliced portions of the signal and reduce noise effect. A Hamming-windowed 1024-point Fast Fourier transform (FFT) for non-overlapping windows of 2000 samples (5.0 seconds) in the range of 0-200 Hz, yielding a frequency resolution of approximately 0.39 Hz, generated two dimensional graph displaying the power (μV^2) of a particular frequency component in a signal. Then, we calculated mean of 10 PSDs (range 0.39 to 30 Hz) using Microsoft Excel 2013 software.

2.6 Histological analysis

Five days after infusion, animals were sacrificed, brains were removed and placed in a fixing solution overnight and used for the morphological evaluation. Rat brains were fixed in Carnoy's solution (ethanol 60%, chloroform 30% and glacial acetic acid 10%), embedded in paraffin, cut in 10 μm tissue sections mounted on slides and collected for histology and immunohistochemistry.

Histological analysis were performed by a trained observer which was blinded to the treatment and to the severity of seizures.

2.6.1 Nissl staining

For morphological analysis (including cell density analysis) deparaffinized sections were processed for Nissl staining. Briefly, slides were stained with thionine acetate solution (Carlo Erba Reagents, Rodano, MI, Italy) for 8 minutes and then washed with distilled water. The sections were mounted with coverslips and analysed with optical microscope.

2.6.2 Fluoro-Jade B staining

Fluoro-Jade B (**FJB**) is a **fluorescein** derivative used for histological staining of degenerating neurons (Schmued and Hopkins, 2000). The slides were incubated with 0.06% potassium permanganate for 10 minutes at room temperature and then washed with distilled water. Sections were incubated with 0.0004% Fluoro-Jade B solution (Merck Millipore) (in a solution of acetic acid

0.01%) at room temperature for 20 minutes, and then slides were mounted with coverslips and analysed with fluorescence microscope (Axiophot Image, Zeiss).

2.6.3 Immunohistochemistry

Tissue sections were deparaffinized and antigen retrieval was performed with citrate buffer pH 6.0 (for anti-HSP-70 antibody) or with buffer pH 8.0 [for anti-Choline acetyltransferase (ChAT) antibody] for 10 minutes. The sections were incubated with 0.01% Triton X-100 (Sigma Aldrich) for 15 minutes and were soaked in 3% hydrogen peroxide to block endogenous peroxidase activity; then were incubated overnight at +4°C with mouse monoclonal mouse anti-HSP-70 (1:100; R&D Systems, Minneapolis, MN, Canada; RRID: AB_211938) or rabbit anti-ChAT antibodies (1:100; Merck Millipore, Billerica, MA, USA; RRID: AB_2079760); the sections were incubated with anti-mouse (RRID:AB_2313581) or anti-rabbit (RRID:AB_2313606) biotinylated secondary antibodies (1:200; Vector Laboratories, Burlingame, CA, USA) for 1 hour at room temperature. The sections stained with anti-HSP-70 antibodies were counterstained with Mayer's Haematoxylin (Diapath, Martinengo, BG, Italy) for 6 minutes, washed with distilled water for 6 minutes and dehydrated. **Sections stained with anti-HSP-70 were used only for qualitative assessments, while the sections stained with anti-ChAT antibodies were used for quantitative data (see below).**

2.6.4 Neuronal cell density

Neuronal cell density values (number of neurons/mm²) were calculated in brain tissue slides stained with Nissl, with ChAT and with FJB. Nissl- and ChAT-positive neurons were counted within a square (dissector) of known dimension (50 x 50 μm) as previously described (Motolese et al., 2015). In brief, dissectors are randomly placed by a software (Image Pro Plus 6.2) within an area of interest, drawn by the operator at low magnification (2.5x) over the various regions analyzed. Inside each dissectors, at high magnification (100x), the operator counts all the neurons falling within it. The results were expressed as the cell density per mm². Four anatomical levels (coupled by level) for each animal were counted starting from level 0.48 mm to -1.80 mm.

For FJB-positive cells count we have selected 5 microscopic fields per slice for 4 levels per animal with software ImageJ within an area of interest. The magnification used for fluorescence counts is 10x over the various regions analyzed. For each microscopic field the operator counts all the positive neurons he sees inside the field. The results were expressed as the cell density per mm². The sections were spaced 50 microns apart (Yamaguchi and Shen, 2013).

2.7 Statistical Analysis

Comparisons among the different groups were performed with two way [seizure group (vehicle/low severity/high severity) x brain side analyzed] Analysis of Variance (ANOVA) with Bonferroni post-hoc analysis.

Null hypothesis was rejected for $p < 0.05$.

3. Results

3.1 Seizures and SE.

Rats that did not show seizures or experienced only sporadic focal seizures (N = 12), or died before microinfusion (N = 9) were not included in the study; 5 rats were excluded because, even though they showed seizures/SE, infusion cannula was not verified as correctly placed in the APC (**most of them showed only stage 0,5-1 isolated seizures during a period of few minutes, one rat showed a few episodes of SE, with total seizure period of approximately 40 min**). All of the remaining rats microinfused with bicuculline+cyclothiazide experienced SE (4 of which were used for EEG recording), but 5 died during SE or in the 24h following it. **Thus ten rats with SE were used for the final morphological analysis. All of the five rats microinfused with saline into the APC were included in results, as in all of them the cannula was correctly placed and none of them showed any seizure after infusion.**

In rats in which morphological analysis were performed, the mean latency to seizure was 5 ± 2 min; 5 rats showed a medium seizure score ≤ 2 , while it was > 2 in the remaining 5 rats; these groups were classified as “low” and “high” severity seizure score, respectively. **The mean of the mean seizure scores of the rats of the low severity score group was $1,70 \pm 0,1$, while it was $3,2 \pm 0,27$ for the high severity score group. Some rats from the high severity score experienced isolated periods of score 5 seizures.** The mean SE duration was $235 \text{ min} \pm 22 \text{ min}$, and not statistically different between the two seizure severity groups (low severity = $206 \text{ min} \pm 34 \text{ min}$; high severity $249 \text{ min} \pm 19 \text{ min}$). **Even though the precise number of seizures were not recorded during the observation, in general we observed that rats belonging to the two severity groups showed a similar incidence of behavioral seizures throughout the seizure period.** Behavioral observation of different types of SE was roughly corresponding to different EEG features in those rats which had been submitted to ESCoG recording. In fact, during seizures with behavioral score > 2 , epileptiform activity was bilateral, composed of sub-continuous/continuous bi-hemispheric spikes and spike-wave activity. During low-severity seizure score, EEG was represented by recurrent, intermittent spike/spike-wave activity, often with a prevalence in the left hemisphere, but also spreading contralaterally. Such a visual difference was confirmed by power spectrum analysis, showing markedly different patterns, with a highest power, and highest frequency bands, for rats with more severe seizures (**Fig. 1**).

3.2. Neuronal loss after SE in limbic structures

Compared with saline-infused animals, in the whole population of rats experiencing SE, there was significant neuronal loss in the APC of the infused side. Such a difference was not significant in the contralateral APC **in the low seizure group**, but reached statistical significance in animals experiencing high severity seizure score (**Fig. 2**).

At the level of the hippocampus, a significant pyramidal cell loss was observed in the CA1, CA3 regions both ipsilaterally and contralaterally to APC infusions in all **groups of animals with SE independently of the severity score, and** this phenomenon was particularly severe, both ipsi-and

contra-laterally to the infusion site, in rats having seizure score > 2 , both in CA1 and CA3 regions (**Fig. 3**). Neuronal loss was significantly higher ipsilaterally than contralaterally to the infusion site both in CA 1 and CA3, both in low- and high severity SE. In high severity score SE group, the neuronal loss was significantly higher than in the low-severity score SE group, both ipsi- and contralaterally to the infusion site in both regions (**Fig. 3**).

3.3. Neuronal loss after SE in basal forebrain cholinergic nuclei.

SE induced a marked, significant cholinergic neuron loss in the NBM ipsilaterally to the site of infusion both in low- and high-severity score SE group, and, to a lesser extent, also contralaterally in the two severity groups. The ipsilateral hemisphere was more affected than the contralateral one within each severity group even though this effect was not significant (**Fig. 4**).

Concerning the cholinergic neurons of MSN, there was a significant cell loss in the SE group irrespective of the seizure severity group, and similar for the two hemispheres (**Fig. 4**).

Finally, concerning DBB, we observed a significant neuronal loss in both hemispheres, both in low-severity and high-severity score SE groups, without significant inter-hemispheric differences within each severity group. In both hemispheres, the neuronal loss was higher in the high-severity score group vs. low severity one (**Fig. 4**).

3.4 Fluoro-Jade B staining after SE

FJB staining in rats with seizure score ≤ 2 confirmed neurodegenerative phenomena not only in the ipsilateral APC, **but also contralaterally** (**Fig. 5**); this phenomenon was even higher in the high severity group, where there was a slight, not significant, prevalence of FJB-positive neurons in the ipsilateral cortex (**Fig. 5**). In the hippocampal CA3 region a significant number of FJB-positive neurons could be detected in low- severity score SE ipsi-and contralaterally to the site of infusion, and this effect was even more marked in the high severity score group (**Fig. 6**). In the NBM a significant number of FJB-positive neurons could be observed ipsilaterally to the site of infusion in the low severity group and, to a higher extent, in the high severity group. In the latter group a

significant occurrence of FJB-positive neurons could be found also contralaterally, but still lower than in the ipsilateral NBM (**Fig. 7**). Concerning MSN, here a marked increase could be observed, ipsilaterally to the infused APC in the high severity group, and, to a lesser extent, also contralaterally (**Fig. 8**). **A similar effect was shown for the DBB (Fig. 9) and in the ventromedial thalamic nucleus (Fig. 10).**

In rats infused with saline no Fluoro-Jade positive neurons were observed in above-mentioned regions.

3.5 Effects of SE on HSP-70 expression

HSP-70 was expressed at the level of the APC (**Fig. 11**) and hippocampus (**Fig. 12**), mainly ipsilaterally to the site of infusion. HSP-70 immunohistochemistry showed an increased expression also in both the NBM and MSN; this was massive in rats experiencing high severity SE, but it was observed also in rats experiencing low severity SE score (**Fig. 13**).

4. Discussion

In this study we profited from a model of “purely focally-induced status epilepticus” to determine the brain areas where cell loss occurs following seizure activity. In fact, when a blocker of AMPA receptor desensitization is microinfused within the anterior piriform cortex prior to picomolar doses of bicuculline a prolonged status epilepticus occurs which becomes independent by the seizure triggering and self-sustaining for several h **often spreading to motor cortex** (Fornai et al., 2000). Apart from classic limbic regions, brain damage was analyzed at the level of basal forebrain cholinergic nuclei, namely NBM, MSN and DBB. In particular, an ipsilateral damage was observed at the level of all the three nuclei, even when considering rats with lower seizure severity score. The contralateral MSN and DBB nuclei were already significantly affected both in the low severity and high severity score groups, with a higher effect in the DBB. The extent of cell loss was similar

in the two hemispheres within each seizure severity group for MSN and DBB, while at the level of NBM it was slightly higher in the ipsilateral vs contralateral one in the low severity group. The cell loss within cholinergic nuclei occurred in parallel with neuronal loss into the APC itself, and hippocampus, which is anatomically connected with the seizure trigger site (Gale, 1992).

Degenerative phenomena in these cholinergic areas, similarly to what observed in the hippocampus, APC and thalamus, were confirmed by Fluoro-Jade B analysis. Finally, the expression of HSP-70 was increased in the APC, hippocampus and cholinergic nuclei. HSP-70 is a heat-shock protein, which, by acting as chaperon, might represent a potential of stress-induced neurodegenerative phenomena (e.g. Lu et al., 2010) as it has been reported in experimental limbic seizures (Chang et al., 2014). Consistently, an increase of circulating HSP-70 has been proposed, in humans, as a potential biomarker of seizure-related brain injury (Rejdak et al., 2012).

SE evoked from the APC represents a model of SE in which seizures triggered focally, in a region roughly corresponding to the primary olfactory cortex, close to the periamygdaloid human cortex, spread to other subcortical and cortical regions throughout the natural anatomical pathways connecting these areas to one another (Fornai et al., 2005; Giorgi et al., 2008). This resembles what can happen also in patients experiencing focal seizures and SE, in which a focal seizure triggering lesion can be present at the level of limbic structures, and seizures can propagate to other brain areas up to secondary generalisation. This model overcomes the potential bias which may derive from the most commonly used rodent models of SE, such as those induced by intraperitoneal administration of either kainic acid or pilocarpine, which affect the whole brain at the same time, independently by the concomitant seizure spreading. Thus, the phenomena we observed in the present study in different parts of the brain can be considered the effects of the sole propagation of seizure activity for prolonged time intervals.

We confirmed that in animals experiencing severe APC-triggered SE there is a damage at the level of the hippocampus CA1 and CA3, resembling the so-called Ammon's horn sclerosis (AHS) described in patients affected by TLE (see also Giorgi et al., 2003; 2006). TLE itself has been

interpreted by several authors as the effect of a remote episode of repeated limbic seizures, giving rise to secondary epileptogenesis, associated with AHS (Cendes et al., 1993; see also Sloviter, 2008). The present model adds new evidence to this hypothesis. **Several rat models of SE triggered from limbic structures have been produced in the last decades, such as the intraamygdaloid kainate (Ben-Ari et al., 1979; 1980), the intrahippocampal Kainate (Schwarcz et al., 1978) or pilocarpine (Furtado et al., 2011; Castro et al., 2011), and the self-sustaining limbic SE induced by continuous hippocampal electrical stimulation (Lothman et al., 1989). All of these models produce prolonged seizures/SE, which are sometimes mainly represented by focal limbic/motor episodes (Lothman et al., 1989) up to sub-continuous generalized tonic-clonic ones (Ben-Ari et al., 1983). In most of these models only the ipsilateral hippocampus was morphologically assessed, and showed constantly signs resembling human AHS (Bertram et al., 1990; Bertram and Lothman., 1993; French et al., 1982; Furtado et al., 2011; Rattka et al., 2013). Ben-Ari et al. (1983), assessed the whole brain at 4 days after intraamygdaloid kainate infusion and showed bilateral amygdaloid, hippocampal, and thalamic neuronal necrosis (Ben-Ari et al., 1983). We also observed bilateral limbic alterations, together with degenerative phenomena also in the thalamus, and alterations in cholinergic nuclei; the latter were not assessed by Ben-Ari et al. (1983). In any case, as said, the SE induced by their intraamygdaloid protocol is featured by sub-continuous generalized convulsive seizures (often stage V as defined in this paper), i.e. significantly more severe than those experienced by most of the rats assessed in the present study.**

Several studies in the last decades have shown the presence of subtle cognitive alterations in TLE patients (e.g., see review by Bell et al., 2011). In the clinical setting it is often difficult to establish whether such an impairment is due either to pre-morbid predisposition, or to a prolonged treatment with antiepileptic drugs (most of which bear cognitive effects), or to degenerative effects due to the seizure themselves.

Furthermore, all of the above potential confounding effects are present also concerning the *sequelae* of SE, and this explains why there are no specific data on this issue in patients with previous SE.

In this study we showed that NBM, MSN and DBB undergo significant cell loss as a consequence of pure and prolonged spreading of seizure activity. This effect is likely to be related to the strict anatomical connections existing between limbic cortex and these cholinergic nuclei. In fact, NBM and MSN receives direct afferents from the piriform cortex (Mesulam and Mufson, 1984; Mesulam, 2013), the MSN and DBB receive afferents mainly from the hippocampus (Haghdoust-Yazdi et al., 2009). The apparent discrepancy that, the already in the group with low severity SE there was a strong contralateral cell loss in MSN, and even more in DBB, compared with NBM, might be due to the higher connection of DBB and MSN with the hippocampus via commissural pathway (e.g. Finnerty and Gefferys, 1993). In fact, in this study the contralateral hippocampus was damaged as well, and this is in line with the occurrence of contralateral AHS in patients with TLE who experience severe and frequent seizures (Meencke et al., 1996). A faster involvement of the contralateral sides for DBB and MSN might also explain, at least in part, the fact that, in the low severity group FJB neurons were less represented in both nuclei, compared with NBM: in these nuclei cell loss could have been already occurred at the time of sacrifice due to the massive recruitment of those areas by SE.

Cholinergic neurons in NBM, MSN and DBB bear important roles in cognitive functions, and especially in memory consolidation and attention (Schliebs and Arendt, 2011). While NBM extensively innervate the whole neocortex, limbic cortices are innervated by MSN and DBB, and the latter is the main source of cholinergic afferents to the hippocampus. Thus, the involvement of basal forebrain cholinergic nuclei might concur, together with the limbic degenerative effects described above, to the cognitive alterations observed in TLE patients. **We could not assess the cognitive outcome in the rats submitted to SE, and thus the potential effects on cognition of the model of SE evoked from APC is speculative; a behavioural study in which cognitive performance impairment are correlated with the impairment of cholinergic (and other ones)**

regions would answer to this question. In any case there are several hints for a significant delayed effect of SE on cognition in humans, and this experimental approach might help to overcome the limits of studies in patients (mainly the potential role on cognition of the etiology of SE itself) (e.g. see the observations by Dodrill and Wilensky, 1990; Helmstaedter, 2007). Incidentally, among the other abovementioned focal models of SE of limbic origin, chronic cognitive performances have been tested rarely (e.g. Rattka et al., 2013, for intrahippocampal kainic acid) and learning and memory impairment has been analyzed only in parallel with hippocampal alterations, and no other brain structures (including cholinergic nuclei) have been assessed.

Recently, Soares et al. (2017), showed that in rats treated with KA or pilocarpine, SE was associated with chronic increase in cholinergic neuron density and number and cell volume in the MSN and DBB. These data are not directly comparable with the present study since SE was induced by systemic chemoconvulsants instead of being evoked within a limbic cortex. Nonetheless such a discrepancy may be further interpreted since both pilocarpine and KA affect directly different nuclei, including MSN/DBB. Moreover, in the study by Soares et al. (2017) rats were sacrificed at 90 days after SE, and the increase of neuronal volume might represent the effect of a damage in the same area. Similarly, the chronically increased cholinergic innervations these authors observed in the hippocampus, might represent the effect of a re-innervation after an early damage. The findings by Correia et al. (1998) support this hypothesis, since these authors showed that months after the onset of pilocarpine-induced SE, p75NTR-containing cholinergic neurons at the level of the septal/diagonal band region undergo a significant shrinkage in pilocarpine-induced chronic epilepsy

In humans, an elegant high-resolution MRI study by Butler et al. (2013) demonstrated that septal nuclei are enlarged in patients with TLE (without AHS), as opposed to patients with extra-temporal epilepsy. Accordingly, these Authors hypothesize that these phenomena are due to chronic plasticity leading to an increased activity of spared cells within these nuclei. Of course, as stated by

the authors themselves, these imaging studies do not allow to detect an actual increase in cell bodies/neuron density of these nuclei; in our opinion it might be also postulated that such MRI-detected increase in septal nuclear size might depend also on delayed neuronal alterations and concomitant astrogliosis.

Remarkably, a recent study by Motelow et al (2015) showed that, during focal hippocampal electrically-induced seizures, a decreased activity of basal forebrain cholinergic activity takes place. This was witnessed by reduced cortical ACh release which was concomitant to an increased slow-wave EEG activity. In keeping with this, the authors suggest that this effects may justify why limbic seizures are associated with altered consciousness. **The same group further strengthened this hypothesis by showing a reduction of EEG delta activity associated with focally evoked limbic seizures, by activating tegmental cholinergic neurons by optogenetics approach (Furman et al., 2015).**

It is worth of mentioning that, especially limbic seizures show an higher incidence and might often precede the onset of mild cognitive impairment and frank dementia (Vossel et al., 2017; Cretin et al., 2016). This was often interpreted as a lower seizure triggering threshold which might occur in the presence of early AD-related neuropathology; nonetheless, early hyperexcitability and seizure activity in limbic structures was described to be crucial in triggering and perpetrating the molecular pathways sustaining the neuropathology dementia (Sanchez et al., 2012; Palop and Mucke, 2009).

As one of the well-established alterations in the brains of AD patients is the degeneration of MBN and septal nuclei (Mesulam, 2013), the abovementioned observations offer a fascinating framework in which the observations of the present study of a seizure-induced impairment of basal forebrain cholinergic structures might easily fit.

Funding

This work was supported by Ricerca Corrente from Ministero della Salute.

References

Bazil, C.W., Anderson, C.T., 2001. Sleep structure following status epilepticus. Sleep Med. 2(5), 447-449.

Bell, B., Lin, J.J., Seidenberg, M., Hermann, B., 2011. The neurobiology of cognitive disorders in temporal lobe epilepsy. *Nat. Rev. Neurol.* 7(3), 154-164.

Ben-Ari, Y., Lagowska, J., Tremblay, E., Le Gal La Salle, G.,1979. A new model of focal status epilepticus: intra-amygdaloid application of kainic acid elicits repetitive secondarily generalized convulsive seizures. Brain Res. 163(1), 176-179.

Ben-Ari, Y., Tremblay, E., Ottersen, O.P., 1980. Injections of kainic acid into the amygdaloid complex of the rat: an electrographic, clinical and histological study in relation to the pathology of epilepsy. Neuroscience 5(3), 515-528.

Bertram, E.H., Lothman, E.W., Lenn, N.J., 1990. The hippocampus in experimental chronic epilepsy: a morphometric analysis. Ann Neurol. 27(1), 43-48.

Bertram, E.H. 3rd, Lothman, E.W., 1993. Morphometric effects of intermittent kindled seizures and limbic status epilepticus in the dentate gyrus of the rat. Brain Res. 603(1), 25-31.

Butler, T., Zaborszky, L., Wang, X., McDonald, C.R., Blackmon, K., Quinn, B.T., DuBois, J., Carlson, C., Barr, W.B., French, J., Kuzniecky, R., Halgren, E., Devinsky, O., Thesen, T., 2013. Septal nuclei enlargement in human temporal lobe epilepsy without mesial temporal sclerosis. *Neurology* 80(5), 487-491.

Buzsaki, G., Bickford, R.G., Ponomareff, G., Thal, L.J., Mandel, R., Gage, F.H., 1988. Nucleus basalis and thalamic control of neocortical activity in the freely moving rat. *J. Neurosci.* 8(11), 4007-4026.

Cassidy, R.M., Gale, K., 1998. Mediodorsal thalamus plays a critical role in the development of limbic motor seizures. *J Neurosci.* 18(21), 9002-9009.

Castro, O.W., Furtado, M.A., Tilelli, C.Q., Fernandes, A., Pajolla, G.P., Garcia-Cairasco, N..2011. Comparative neuroanatomical and temporal characterization of FluoroJade-positive neurodegeneration after status epilepticus induced by systemic and intrahippocampal pilocarpine in Wistar rats. *Brain Res.* 1374, 43-55.

Cendes, F., Andermann, F., Gloor, P., Lopes-Cendes, I., Andermann, E., Melanson, D., Jones-Gotman, M., Robitaille, Y., Evans, A., Peters, T.,1993. Atrophy of mesial structures in patients with temporal lobe epilepsy: cause or consequence of repeated seizures? *Ann. Neurol.* 34(6), 795-801.

Chang, C.C., Chen, S.D., Lin, T.K., Chang, W.N., Liou, C.W., Chang, A.Y., Chan, S.H., Chuang, Y.C., 2014. Heat shock protein 70 protects against seizure-induced neuronal cell death in the hippocampus following experimental status epilepticus via inhibition of nuclear factor- κ B activation-induced nitric oxide synthase II expression. *Neurobiol. Dis.* 62, 241-249.

Correia, L., Amado, D., Cavalheiro, E.A., Bentivogliom M., 1998. Persistence and atrophy of septal/diagonal band neurons expressing the p75 neurotrophin receptor in pilocarpine-induced chronic epilepsy in the rat. *Brain Res.* 809(2), 288-293.

Cretin, B., Sellal, F., Philippi, N., Bousiges, O., Di Bitonto, L., Martin-Hunyadi, C., Blanc, F., 2016. Epileptic Prodromal Alzheimer's Disease, a Retrospective Study of 13 New Cases:

Expanding the Spectrum of Alzheimer's Disease to an Epileptic Variant? *J. Alzheimers Dis.* 52(3), 1125-1133.

Dage, R.C.A., 1979. Centrally mediated prolonged hypotension produced by oxotremorine or pilocarpine *Br J Pharmacol.* 65(1), 15–21.

Dodrill, C.B., Wilensky, A.J., 1990. Intellectual impairment as an outcome of status epilepticus. *Neurology.* 40(5 Suppl 2), 23-27.

Dybdal, D., Gale, K. 2000. Postural and anticonvulsant effects of inhibition of the rat subthalamic nucleus. *J. Neurosci.* 20(17), 6728-6733.

Everitt, B.J., Robbins, T.W., 1997. Central cholinergic systems and cognition. *Ann. Rev. Psychol.*, 48, 649-684.

Finnerty, G.T., Jefferys, J.G.R., 1993. Functional connectivity from CA3 to the ipsilateral and contralateral CA1 in the rat dorsal hippocampus, *Neuroscience* 56, 101-108.

Fornai, F., Bassi, L., Gesi, M., Giorgi, F.S., Guerrini, R., Bonaccorsi, I., Alessandri, M.G., 2000. Similar increases in extracellular lactic acid in the limbic system during epileptic and/or olfactory stimulation. *Neuroscience* 9, 447-458.

Fornai, F., Busceti, C.L., Kondratyev, A., Gale, K., 2005. AMPA receptor desensitization as a determinant of vulnerability to focally evoked status epilepticus. *Eur. J. Neurosci.*, 21, 455-463.

French, E.D., Aldinio, C., Schwarcz, R., 1982. Intrahippocampal kainic acid, seizures and local neuronal degeneration: relationships assessed in unanesthetized rats. *Neuroscience*. 7(10), 2525-2536.

Furman, M., Zhan, Q., McCafferty, C., Lerner, B.A., Motelow, J.E., Meng, J., Ma, C., Buchanan, G.F., Witten, I.B., Deisseroth, K., Cardin, J.A., Blumenfeld, H., 2015. Optogenetic stimulation of cholinergic brainstem neurons during focal limbic seizures: Effects on cortical physiology. *Epilepsia*. 56(12), e198-e202.

Furtado, M.A., Braga, G.K., Oliveira, J.A., Del, V.F., Garcia-Cairasco, N. 2002. Behavioral, morphologic, and electroencephalographic evaluation of seizures induced by intrahippocampal microinjection of pilocarpine. *Epilepsia*, 43 (S5), 37-39.

Furtado, M.A., Castro, O.W., Del Vecchio, F., de Oliveira, J.A, Garcia-Cairasco, N., 2011. Study of spontaneous recurrent seizures and morphological alterations after status epilepticus induced by intrahippocampal injection of pilocarpine. *Epilepsy Behav*. 20(2), 257-266.

Gale, K., 1992. Subcortical structures and pathways involved in convulsive seizure generation. *J. Clin. Neurophysiol*. 9(2), 264-277.

Giorgi, F.S., Ferrucci, M., Lazzeri, G., Pizzanelli, C., Lenzi, P., Alessandri, M.G., Murri, L., Fornai, F., 2003. A damage to locus coeruleus neurons converts sporadic seizures into self-sustaining limbic status epilepticus. *Eur. J. Neurosci*. 17, 2593-2601.

Giorgi, F.S., Mauceli, G., Blandini, F., Ruggieri, S., Paparelli, A., Murri, L., Fornai, F., 2006. Locus coeruleus and neuronal plasticity in a model of focal limbic epilepsy. *Epilepsia* 47 (suppl. 5), 21-25.

Giorgi, F.S., Blandini, F., Cantafora, E., Biagioni, F., Armentero, M.T., Pasquali, L., Orzi, F., Murri, L., Paparelli, A., Fornai, F., 2008. Activation of brain metabolism and fos during limbic seizures: the role of locus coeruleus. *Neurobiol. Dis.* 30(3), 388-399.

Haghdoust-Yazdi, H., Pasbakhsh, P., Vatanparast, J., Rajaei, F., Behzadi, G., 2009. Topographical and quantitative distribution of the projecting neurons to main divisions of the septal area. *Neurol. Res.* 31(5), 503-513.

Halonen, T., Tortorella, A., Zrebeet, H., Gale, K., 1994. Posterior piriform and perirhinal cortex relay seizures evoked from the area tempestas: role of excitatory and inhibitory amino acid receptors. *Brain Res.* 652(1), 145-148.

Helmstaedter, C., 2007. Cognitive outcome of status epilepticus in adults. *Epilepsia.* 48(8), 85-90.

Lagos, P., Monti, J.M., Jantos, H., Torterolo, P., 2012. Microinjection of the melanin-concentrating hormone into the lateral basal forebrain increases REM sleep and reduces wakefulness in the rat. *Life Sci.* 90(23-24), 895-899.

Lanaud, P., Maggio, R., Gale, K., Grayson, D.R., 1993. Temporal and spatial patterns of expression of c-fos, zif/268, c-jun and jun-B mRNAs in rat brain following seizures evoked focally from the deep prepiriform cortex. *Exp. Neurol.* 119(1), 20-31.

Lau, A., Tymianski, M., 2010. Glutamate receptors, neurotoxicity and neurodegeneration. *Pflugers Arch.* 460(2), 525-542

Lothman, E.W., Bertram, E.H., Bekenstein, J.W., Perlin, J.B., 1989. Self-sustaining limbic status epilepticus induced by 'continuous' hippocampal stimulation: electrographic and behavioral characteristics. *Epilepsy Res.* 3(2), 107-119.

Lu, T.Z., Quan, Y., Feng, Z.P., 2010. Multifaceted role of heat shock protein 70 in neurons. *Mol. Neurobiol.* 42, 114-123.

Maggio, R., Gale, K., 1989. Seizures evoked from area tempestas are subject to control by GABA and glutamate receptors in substantia nigra. *Exp. Neurol.* 105(2), 184-188.

Maggio, R., Lanaud, P., Grayson, D.R., Gale, K., 1993. Expression of c-fos mRNA following seizures evoked from an epileptogenic site in the deep prepiriform cortex: regional distribution in brain as shown by in situ hybridization. *Exp. Neurol.* 119(1), 11-19.

Meencke, H.J., Veith, G., Lund, S., 1996. Bilateral hippocampal sclerosis and secondary epileptogenesis. *Epilepsy Res. Suppl.* 12, 335-342.

Mesulam, M.M., Mufson, E.J., Wainer, B.H., Levey, A.I., 1983a. Central cholinergic pathways in the rat: an overview based on an alternative nomenclature (Ch1-Ch6). *Neuroscience* 10(4), 1185-1201.

Mesulam, M.M., Mufson, E.J., Levey, A.I., Wainer, B.H., 1983b. Cholinergic innervation of cortex by the basal forebrain: cytochemistry and cortical connections of the septal area, diagonal band nuclei, nucleus basalis (substantia innominata), and hypothalamus in the rhesus monkey. *J. Comp. Neurol.* 214(2), 170-197.

Mesulam, M.M., Mufson, E.J., 1984. Neural inputs into the nucleus basalis of the substantia innominata (Ch4) in the rhesus monkey. *Brain* 107 (Pt 1), 253-274.

Mesulam M.M., 2013. Cholinergic circuitry of the human nucleus basalis and its fate in Alzheimer's disease. *J. Comp. Neurol.* 521(18), 4124-4144.

Motelow, J.E., Li, W., Zhan, Q., Mishra, A.M., Sachdev, R.N., Liu, G., Gummadavelli, A., Zayyad, Z., Lee, H.S., Chu, V., Andrews, J.P., Englotm D.J., Hermann P., Sanganahalli, B.G., Hyder, F., Blumenfeld, H.. 2015. Decreased subcortical cholinergic arousal in focal seizures. *Neuron* 85(3), 561-572.

Motolese, M., Mastroiacovo, F., Cannella, M., Bucci, D., Gaglione, A., Riozzi, B., Lütjens, R., Poli, S.M., Celanire, S., Bruno, V., Battaglia, G., Nicoletti, F. 2015. Targeting type-2 metabotropic glutamate receptors to protect vulnerable hippocampal neurons against ischemic damage. *Mol. Brain*, 8(1), 66. doi: 10.1186/s13041-015-0158-2

Nitecka, L., Tremblay, E., Charton, G., Bouillot, J.P., Berger, M.L., Ben-Ari, Y., 1984. Maturation of kainic acid seizure-brain damage syndrome in the rat. II. Histopathological sequelae. *Neuroscience* 13(4), 1073-1094.

Palop, J.J., Mucke, L., 2009. Epilepsy and cognitive impairments in Alzheimer disease. *Arch. Neurol.* 66(4), 435-440.

Panayiotopoulos, C.P., 2002. *A Clinical Guide to Epileptic Syndromes and their Treatment: Based on the New ILAE Diagnostic Scheme*, first ed. Bladon Medical Publishing, Limited, Oxfordshire, UK.

Paxinos, G., Watson, C., 1997. *The Rat Brain in Stereotaxic Coordinates*, 3rd ed. Academic Press, San Diego, U.S.A.

Pellegrino, L.J., Pellegrino, A.S., Cushman, A.J., 1979. *A Stereotaxic Atlas of the Rat Brain*, second ed. Plenum Press, New York.

Piredda, S., Gale, K., 1985. Evidence that the deep prepiriform cortex contains a crucial epileptogenic site. *Nature* 317, 623-625.

Power, K.N., Gramstad, A., Gilhus, N.E., Hufthammer, K.O., Engelsen, B.A., 2018. Cognitive dysfunction after generalized tonic-clonic status epilepticus in adults. *Acta Neurol Scand.* 137, 417-424.

Racine, R., 1972. Modifications of seizure activity by electrical stimulation. II. Motor seizure. *Electroencephalogr. Clin. Neurophysiol.* 32, 281-294.

Rattka, M., Brandt, C., Löscher, W., 2013. The intrahippocampal kainate model of temporal lobe epilepsy revisited: epileptogenesis, behavioral and cognitive alterations, pharmacological response, and hippocampal damage in epileptic rats. *Epilepsy Res.* 103(2-3), 135-152.

Rejdak, K., Kuhle, J., Rüegg, S., Lindberg, R.L., Petzold, A., Sulejczak, D., Papuc, E., Rejdak, R., Stelmasiak, Z., Grieb, P., 2012. Neurofilament heavy chain and heat shock protein 70 as markers of seizure-related brain injury. *Epilepsia* 53(5), 922-7.

Roland, J.J., Stewart, A.L., Janke, K.L., Gielow, M.R., Kostek, J.A., Savage, L.M., Servatius, R.J., Pang, K.C., 2014. Medial septum-diagonal band of Broca (MSDB) GABAergic

regulation of hippocampal acetylcholine efflux is dependent on cognitive demands. *J Neurosci.* 34(2), 506-514.

Sanchez, P.E., Zhu, L., Verret, L., Vossel, K.A., Orr, A.G., Cirrito, J.R., Devidze, N., Ho, K., Yu, G.Q., Palop, J.J., Mucke, L., 2012. Levetiracetam suppresses neuronal network dysfunction and reverses synaptic and cognitive deficits in an Alzheimer's disease model. *Proc. Natl. Acad. Sci. U. S. A.* 109(42), E2895-E2903.

Sarter, M., Bruno, J.P., 1997. Cognitive functions of cortical acetylcholine: toward a unifying hypothesis. *Brain Res. Rev.* 23, 28-46.

Schliebs, R., Arendt, T., 2011. The cholinergic system in aging and neuronal degeneration. *Behav. Brain Res.* 221(2), 555-563.

Schmued, L.C., Hopkins, K.J., 2000. Fluoro-Jade B: a high affinity fluorescent marker for the localization of neuronal degeneration. *Brain Res.* 874(2), 123-130.

Schwarcz, R., Zaczek, R., Coyle, J.T., 1978. Microinjection of kainic acid into the rat hippocampus. *Eur J Pharmacol.* 50(3), 209-220.

Shimosaka, S., So, Y.T., Simon, R.P., 1994. Deep prepiriform cortex modulates kainate-induced hippocampal injury. *Neuroscience* 61(4), 817-822.

Shimosaka, S., So, Y.T., Simon, R.P., 1992. Distribution of HSP72 induction and neuronal death following limbic seizures. *Neurosci. Lett.* 138(2), 202-206.

Sloviter, R.S., 2008. Hippocampal epileptogenesis in animal models of mesial temporal lobe epilepsy with hippocampal sclerosis: the importance of the "latent period" and other concepts. *Epilepsia* 49 Suppl 9, 85-92.

Soares, J.I., Valente, M.C., Andrade, P.A., Maia G.H., Lukoyanov, N.V., 2017. Reorganization of the septohippocampal cholinergic fiber system in experimental epilepsy. *J Comp. Neurol.* 525(12), 2690-2705.

Swanson, L.W., Cowan W.M., 1979. The connections of the septal region in the rat. *J. Comp. Neurol.* 186(4), 621-655.

Szymusiak, R., 1995. Magnocellular nuclei of the basal forebrain: substrates of sleep and arousal. *Sleep* 18, 478-500.

Tortorella, A., Halonen, T., Sahibzada, N., Gale, K., 1997. A crucial role of the alpha-amino-3-hydroxy-5-methylisoxazole-4-propionic acid subtype of glutamate receptors in piriform and perirhinal cortex for the initiation and propagation of limbic motor seizures. *J. Pharmacol. Exp. Ther.* 280(3), 1401-1405.

Tremblay, E., Nitecka, L., Berger, M.L., Ben-Ari, Y., 1984. Maturation of kainic acid seizure-brain damage syndrome in the rat. I. Clinical, electrographic and metabolic observations. *Neuroscience.* 13(4), 1051-1072.

Trinka, E., Cock, H., Hesdorffer, D., Rossetti, A.O., Scheffer, I.E., Shinnar, S., Shorvon, S., Lowenstein, D.H., 2015. A definition and classification of status epilepticus—Report of the ILAE Task Force on Classification of Status Epilepticus. *Epilepsia.* 56(10), 1515-1523.

Turski, W.A., Cavalheiro, E.A., Schwarz, M., Czuczwar, S.J., Kleinrok, Z., Turski, L., 1983. Limbic seizures produced by pilocarpine in rats: behavioural, electroencephalographic and neuropathological study. *Behav. Brain Res.* 9(3), 315-335.

Vismer, M.S., Forcelli, P.A., Skopin, M.D., Gale, K., Koubeissi, M.Z., 2015. The piriform, perirhinal, and entorhinal cortex in seizure generation. *Front. Neural Circuits* 9, 27. doi: 10.3389/fncir.2015.00027.

Vossel, K.A., Tartaglia, M.C., Nygaard, H.B., Zeman, A.Z., Miller, B.L., 2017. Epileptic activity in Alzheimer's disease: causes and clinical relevance. *Lancet Neurol.* 16(4), 311-322.

Yamaguchi, H., Shen, J., 2013. Histological analysis of neurodegeneration in the mouse brain. *Methods Mol Biol.* 1004, 91-113.

Zaborszky, L, van den Pol, A., Gyengesi, E., 2012. Chapter 28: The Basal Forebrain Cholinergic Projection System in Mice. In: *The Mouse Nervous System*, Edited by: Charles Watson, George Paxinos and Luis Puellas,. Academic Press, New York. 2012, 684-718.

Zant, J.C., Kim, T., Prokai, L., Szarka, S., McNally, J., McKenna, J.T., Shukla, C., Yang, C., Kalinchuk, A.V., McCarley, R.W., Brown, R.E., Basheer, R., 2016. Cholinergic Neurons in the Basal Forebrain Promote Wakefulness by Actions on Neighboring Non-Cholinergic Neurons: An Opto-Dialysis Study. *J. Neurosci.* 36, 2057-2067.

Figure legends

Figure 1. Features of seizures evoked from APC.

Representative 5-s epochs of ESCoG recorded simultaneously in a single rat from three cortical areas: **primary** somatosensory cortex (SCx left and right) and left frontal motor cortex (FrCx left) during three behavioral states: **A** - background (BGD) during quiet waking state, **B** - during modified Racine's score 1, and **C** - during modified Racine's score 5.

In **panel A**, it is shown a small-amplitude ESCoG during BGD. In **panel B**, it is shown an ESCoG with mixed pattern of recurrent irregular and/or rhythmic spike-and-wave discharges, more evident in the left hemisphere, during modified Racine's score 1 (myoclonic jerks of contralateral forelimb, in simultaneous video recording). In **panel C**, it is shown a 5-s epoch of high-amplitude ESCoG with subcontinuous spikes and slow waves, during Racine's modified score 5 (bilateral forelimb clonus and rearing with loss of balance on the video recording). Mean power spectral density (PSD) over ten 5-s epochs of ESCoG in the Fr Cx left is shown on the right part of the figure for each one of the three ESCoG shown on the left, respectively. The power distribution of particular frequencies differed between the three behavioural states: the PSD of the ESCoG during BGD shows low-power of frequencies in the theta-alpha ranges; the PSD of the ESCoG during seizure Racine score 1 has a peak at 2-3 Hz corresponded to the frequency of the spike-waves; and the high-powered PSD of the ESCoG during seizures with Racine score 5 has three peaks at 1.6, 4.0 and 6.8 Hz, corresponding to frequencies of the epileptiform activity recorded during the chosen 50-s epoch (10 ESCoG fragments of 5s each).

Figure 2. Neuronal loss in the piriform cortex of rats submitted to focal status epilepticus.

The figure shows data obtained with Nissl staining in the piriform cortex.

Animals were obtained as described in the methods section.

Panel A shows representative photomicrographs from animal injected with saline (vehicle), an animal experiencing low severity score (Median score 2) and a rat experiencing high severity score (Median score 4); images from the hemisphere ipsilateral (Ipsilateral side) and contralateral (Contralateral side) to the infused APC are shown. Scale bar= 200 μ m.

In panel B the graph shows the values of neuronal density (assessed in Nissl-stained sections) at the level of piriform cortex of the 3 groups (vehicle, bicuculine+cyclothiazide low severity, and bicuculine+cyclothiazide high severity) in the two hemispheres (Ipsilateral side and Contralateral side). Two-way ANOVA analysis shows a significant effect for group [F(2,24)=56.10; p<0.0001], for side [F(1,24)=48.49; p<0.0001] and group x side interaction [F(2,24)=13.25; p=0.0001].

Post-hoc analysis shows a significant cell loss in the high severity score and ipsilateral low severity score vs. vehicle; within each severity score group there is a significantly higher cell loss in ipsilateral hemisphere compared with contralateral one.

Detailed p values are reported by symbols in the graph and below, in this legend.

* p<0.0001 vs ipsilateral and contralateral vehicle

p<0.0001 vs. contralateral side, same severity

§ p \leq 0.001 vs. contralateral low severity

p <0.05 vs. contralateral high severity

Fig.3 Neuronal loss in the hippocampus of rats submitted to Status Epilepticus.

The figure shows data obtained with Nissl staining in the CA1 and CA3 regions of the hippocampus. The animals were obtained as described in the methods section.

Panel A shows representative photomicrographs from an animal treated with saline (vehicle), or with bicuculline+cyclothiazide animals that had low severity score (Median score 2) or high severity score (Median score 4); images from the ipsilateral (Ipsilateral side) and contralateral (Contralateral side) hemisphere to the infused APC are shown. Scale bar= 200 μ m.

In panel B the graphs show the values of neuronal density (assessed in Nissl-stained sections) at the level of CA1 and CA3 region of the 3 groups. For CA1 region, Two-way ANOVA analysis shows a significant effect for group [$F(2,24)=827.3$; $p<0.0001$], for side [$F(1,24)=29.65$; $p<0.0001$] and group x side interaction [$F(2,24)=21.34$; $p<0.0001$]. For CA3 region, Two-way ANOVA analysis shows a significant effect for group [$F(2,24)=1361$; $p<0.0001$], for side [$F(1,24)=34.94$; $p<0.0001$] and group x side interaction [$F(2,24)=36.48$; $p<0.0001$].

In CA1, post-hoc analysis shows a significant cell loss in the high severity group and low severity group vs. vehicle in both hemispheres; in the high severity group cell loss is more severe than in the low severity group in both sides; within both high and low severity group, the ipsilateral side is more severely affected than the contralateral side.

In CA3, post-hoc analysis shows the same results as for CA1, with the exception of a similar cell loss in both hemispheres in the high severity group.

Detailed p values are reported by symbols in the graph and below, in this legend.

* $p<0.0001$ vs ipsilateral and contralateral vehicle

$p<0.0001$ vs. contralateral side, same severity

§ $p < 0.0001$ vs ipsilateral and contralateral low severity

Fig. 4 Loss of Choline-acetyltransferase-positive neurons in the Nucleus Basalis of Meynert, Medial Septal Nucleus and Diagonal Band of Broca after status epilepticus.

This figure shows the results of immunohistochemistry for Choline-acetyltransferase (ChAT) in the basal forebrain cholinergic nuclei. The animals were obtained as described in the methods section.

Panel A shows representative photomicrographs of the Nucleus basalis of Meynert (upper panels), of the Medial Septal Nucleus (middle panels) and of Diagonal band of Broca (lower

panels). In this image all three groups analyzed are shown (Vehicle, Median score 2 and Median score 4). Scale bar=200 μm . In detail box, the scale bar corresponds to 30 μm .

In panel B the graphs show the values of neuronal density of ChAT-positive neurons at the level of Nucleus basalis of Meynert (upper graph) Medial septal nucleus (middle graph) or Diagonal Bend of Broca (lower graph). The 3 groups (“vehicle”, “bicuculine+cyclothiazide low severity”, and “bicuculine+cyclothiazide high severity”) in the two hemispheres (“Ipsilateral side” and “Contralateral side”) are shown for each graph.

For Nucleus basalis of Meynert, Two-way ANOVA analysis shows a significant effect for group [F(2,24)=14.16; $p<0.0001$], a significant, but lower, effect for side [F(1,24)=7.130; $p=0.0134$] and a non significant effect of group x side interaction [F(2,24)=2.991; $p=0.069$].

For Medial septal nucleus, Two-way ANOVA analysis shows a significant effect for group [F(2,24)=23.42; $p<0.0001$], but not for side [F(1,24)=0.2157; $p=0.646$] and group x side interaction [F(2,24)=0.6079; $p=0.5527$].

For Diagonal Band of Broca, Two-way ANOVA analysis shows a significant effect for group [F(2,24)=177.5; $p<0.0001$], but not for side [F(1,24)=0.672; $p=0.420$] and group x side interaction [F(2,24)=0.728; $p=0.492$].

In Nucleus basalis of Meynert, post-hoc analysis shows a significant cell loss in the high severity score and low severity score vs vehicle in both hemispheres; in the low-grade group the loss is higher in the ipsilateral hemisphere even though without statistical significance; in the ipsilateral side of the high grade group cell loss is more severe than in the contralateral side of the low severity group.

In the Medial septum nucleus, post-hoc analysis shows a severe and similar cell loss both in the low and high severity group; no differences by side are observed.

Similarly in the diagonal band of Broca the cell loss was similar for both sides within each severity group; the cell loss is higher in the high severity group vs the low severity group.

Detailed p values are reported by symbols in the graph and below, in this legend.

* $p<0.01$ vs ipsilateral and contralateral vehicle

$p < 0.05$ vs. contralateral low severity

** $p < 0.0001$ vs. ipsilateral and contralateral vehicle

§ $p < 0.001$ vs ipsilateral and contralateral low severity

$p < 0.01$ vs. low grade (same side)

Figure 5. Fluoro-Jade B-staining in the piriform cortex of rats submitted to focal Status epilepticus.

The figure shows data obtained with Fluoro-Jade B (FJB) staining in the APC. The animals were obtained as described in the methods section.

In A it is shown a representative photomicrographs from animal injected with saline (vehicle), an animal experiencing low severity score (Median score 2) and a rat experiencing high severity score (Median score 4); images from both hemisphere (ipsi- and contralateral) to the infused APC are shown. Scale bar= 50 μm .

In B the graph shows the values of density of FJB-positive neurons at the level of piriform cortex of the 3 groups. Two-way ANOVA analysis shows a significant effect for group [F(2,24)=161.6; $p < 0.0001$], but not for side [F(1,24)=0.9383; $p = 0.3424$] and group x side interaction [F(2,24)=0.3592; $p = 0.7019$]. Post hoc analysis shows that there is a significant occurrence of FJB-positive neurons in the low severity score and even greater one in the high severity score group; no clear difference by hemisphere within each group could be observed.

Post-hoc analysis shows detailed p values are reported by symbols in the graph and below, in this legend.

* $p < 0.001$ vs. ipsilateral and contralateral vehicle

$p < 0.0001$ vs. ipsilateral and contralateral low severity group

Figure 6. Fluoro-Jade B staining in the hippocampus of rats submitted to focal status epilepticus.

The figure shows data obtained with Fluoro-Jade B (FJB) staining in the hippocampus (CA1+CA3). The animals were obtained as described in the methods section.

Panel A shows representative photomicrographs from an animal injected with saline (vehicle), an animal experiencing low severity score (Median score 2) and a rat experiencing high severity score (Median score 4); images from the hemisphere ipsilateral (Ipsilateral side) and contralateral (Contralateral side) to the infused APC are shown. Scale bar= 50 μ m.

In panel B the graphs show the values of density of FJB-positive neurons at the level of hippocampus (CA1+CA3) region of the 3 groups (vehicle, bicuculine+cyclothiazide low severity, and bicuculine+cyclothiazide high severity) in the two hemispheres (Ipsilateral side and Contralateral side).

Two-way ANOVA analysis shows a significant effect for group [$F(2,24)=178.9$; $p<0.0001$], for side [$F(1,24)=43.09$; $p<0.0001$] and group x side interaction [$F(2,24)=13.93$; $p<0.0001$]. Post-hoc analysis shows a significant FJB-staining low severity group vs. vehicle in both hemispheres, and an even higher density of FJB-positive neuron in the high severity group. Within each severity score group, there is a higher number of FJB-positive neurons in the ipsilateral hemisphere.

Detailed p values are reported by symbols in the graph and below, in this legend.

* $p<0.005$ vs. ipsilateral and contralateral vehicle

$p<0.05$ vs. contralateral side, same severity

§ $p<0.0001$ vs ipsilateral and contralateral high severity

Figure 7. Fluoro-Jade B-staining in the Nucleus Basalis of Meynert of rats submitted to focal Status epilepticus.

The figure shows data obtained with Fluoro-Jade B (FJB) staining in the nucleus basalis of Meynert. Animals were obtained as described in the methods section.

Panel A shows representative photomicrographs from an animal injected with saline (vehicle), an animal experiencing low severity score (Median score 2) and a rat experiencing high

severity score (Median score 4); images from the hemisphere ipsilateral (Ipsilateral side) and contralateral (Contralateral side) to the infused APC are shown. Scale bar= 100 μ m.

In panel B the graphs show the values of density of FJB-positive neurons at the level of Nucleus Basalis of Meynert of the 3 groups considered. Two-way ANOVA analysis shows a significant effect for group [$F(2,24)=340.2$; $p<0.0001$], for side [$F(1,24)=152.9$; $p<0.0001$] and group x side interaction [$F(2,24)=67.73$; $p<0.0001$]. Post-hoc analysis shows a significant FJB-staining in the high severity group, and significant, but smaller increase of FJB-positive cells in the ipsilateral low severity group. FJB are significantly more represented ipsilaterally in both severity groups.

Detailed p values are reported by symbols in the graph and below, in this legend.

* $p<0.0001$ vs. ipsilateral and contralateral vehicle

$p<0.001$ vs. contralateral side (same severity)

§ $p<0.0001$ vs. low severity (same hemisphere)

Figure 8. Fluoro-Jade B-staining in the medial septal nucleus of rats submitted to focal Status epilepticus.

The figure shows data obtained with FJB staining in the Medial Septal Nucleus. Animals were obtained as described in the methods section.

In A shows representative photomicrographs from animal injected with saline (vehicle), an animal experiencing low severity score (Median score 2) and a rat experiencing high severity score (Median score 4); images from the hemisphere ipsilateral (Ipsilateral side) and contralateral (Contralateral side) to the infused APC are shown. Scale bar= 100 μ m.

In B the graphs show the values of density of FJB-positive neurons at the level of medial septal nucleus of all groups of animals.

Two-way ANOVA analysis shows a significant effect for group [$F(2,24)=163.5$; $p<0.0001$], for side [$F(1,24)=106.8$; $p<0.0001$] and group x side interaction [$F(2,24)=67.91$; $p<0.0001$]. Post-

hoc analysis shows a significant increase of FJB-positive neurons in the group with high severity seizure score, and particularly in the hemisphere ipsilateral to the infusion.

Detailed p values are reported by symbols in the graph and below, in this legend.

* $p < 0.0001$ vs. ipsilateral and contralateral vehicle

$p < 0.01$ vs. ipsilateral and contralateral vehicle

** $p < 0.0001$ vs. ipsilateral and contralateral low severity

$p < 0.0001$ vs. contralateral low severity

§ $p < 0.001$ vs. ipsilateral high severity

Figure 9. Fluoro-Jade B-staining of the Diagonal Band of Broca of rats submitted to focal Status epilepticus.

The figure shows data obtained with Fluoro-Jade B staining in the Diagonal Band of Broca.

Animals were obtained as described in the methods section.

In A it is shows representative photomicrographs from vehicle, an animal experiencing low severity score (Median score 2) and a rat experiencing high severity score (Median score 4); images from the hemisphere ipsilateral side and contralateral side to the infused APC are shown. Scale bar= 100 μ m.

In B, the graphs show the values of density of FJB-positive neurons at the level of medial septal nucleus of the 3 groups considered. Two-way ANOVA analysis shows a significant effect for group [$F(2,24)=94.67$; $p < 0.0001$], for side [$F(1,24)=68.32$; $p < 0.0001$] and group x side interaction [$F(2,24)=48.18$; $p < 0.0001$].

Post-hoc analysis revealed a significant marked increase of FJB neurons only in the ipsilateral high seizure score (higher than in saline, and low severity sore, bilaterally), while the increase in the contralateral hemisphere is not significant.

Detailed p values are reported by symbols in the graph and below, in this legend.

* $p < 0.0001$ vs. ipsilateral and contralateral vehicle

**** p<0.0001 vs. ipsilateral and contralateral low severity**

p<0.0001 vs. contralateral high severity

Figure 10. Fluoro-Jade B-staining in the ventromedial thalamic nucleus of rats submitted to focal Status epilepticus.

The figure shows data obtained with Fluoro-Jade B (FJB) staining in the ventromedial thalamic nucleus. Animals were obtained as described in the methods section.

Panel A shows representative photomicrographs from vehicle, an animal experiencing low severity score (Median score 2) and a rat experiencing high severity score (Median score 4); images from both the hemisphere (ipsi and contralateral) to the infused APC are shown. Scale bar= 50 μ m.

In B the graphs show the values of density of FJB-positive neurons at the level of ventromedial thalamic nucleus of all groups of animals. Two-way ANOVA analysis shows a significant effect for group [F(2,24)=88.15; p<0.0001], for side [F(1,24)=6.523; p=0.0174] and group x side interaction [F(2,24)=6.173; p=0.0069]. In the low severity group, we did not find FJB-positive neurons, while this was the case in the high severity group, where this increase was significant vs vehicle and low-severity groups, as shown by post-hoc analysis. Post-hoc analysis also showed that within the high severity group there was a significantly higher number of FJB-positive neurons in the ipsilateral hemisphere. Detailed p values are reported by symbols in the graph and below, in this legend.

*** p<0.0001 vs ipsilateral and contralateral vehicle**

p<0.0001 contralateral side, same severity

§ p< 0.0001 vs ipsilateral and contralateral low severity

Fig. 11. Status epilepticus increases Heat Shock Protein-70 immunostaining in the piriform cortex.

This picture shows Heat Shock Protein-70 (**HSP70**) -positive neurons in the piriform cortex of the hemisphere ipsilateral (right column) and contralateral (left column) to the site of infusion, in a saline-injected animal (**Vehicle**, first row), in an animal with low severity seizure score (Median score 2, second row) and in an animal with a high severity seizure score (Median score 4, third row) Status Epilepticus. After status epilepticus, HSP-70 protein expression can be observed in the ipsilateral piriform cortex of rats with medium severity score, and both ipsi- and contralaterally in the piriform cortex of rats with high severity seizure score.

Scale bar =200 μm . In detail box, the scale bar corresponds to 30 μm .

Fig. 12. Status epilepticus increases Heat Shock Protein-70 immunostaining in the hippocampus.

This picture shows Heat Shock Protein-70-positive neurons in the hippocampus of the hemisphere ipsilateral (right column) and contralateral (left column) to the site of infusion, in a saline-injected animal (**Vehicle**, first row), in an animal with low severity seizure score (Median score 2, second row) and in an animal with a high severity seizure score (Median score 4, third row) status epilepticus. After status epilepticus, HSP-70 protein expression can be observed in the ipsilateral hippocampus of rats with medium severity score, and both ipsi- and contralaterally in the hippocampus of rats with high severity seizure score.

Scale bar =200 μm . In detail box, the scale bar corresponds to 30 μm .

Figure 13. Status epilepticus increases Heat Shock Protein-70 immunostaining in the Nucleus Basalis of Meynert and Medial Septal Nucleus.

The Figure shows a representative figure of the expression of Heat shock protein-70 in the Medial Septal Nucleus (left column) and Nucleus Basalis of Meynert (right column) of the hemisphere ipsilateral to the site of infusion, in a saline-injected animal (**Vehicle**), in an animal with low severity seizure score (Median score 2) and in an animal with a high severity seizure score (median score 4) status epilepticus. After Status Epilepticus, HSP-70 positive cells can be observed both in

the medial septum and in the Nucleus Basalis of Meynert. In the medial septum there is a net increase in HSP-70 expression from a low severity to a high severity score; in the Nucleus basalis of Meynert there is already a significant expression of HSP-70 protein in rats with a low severity SE score.

Scale bar=200 μm . In detail box, the scale bar corresponds to 30 μm .

Figure 1
[Click here to download high resolution image](#)

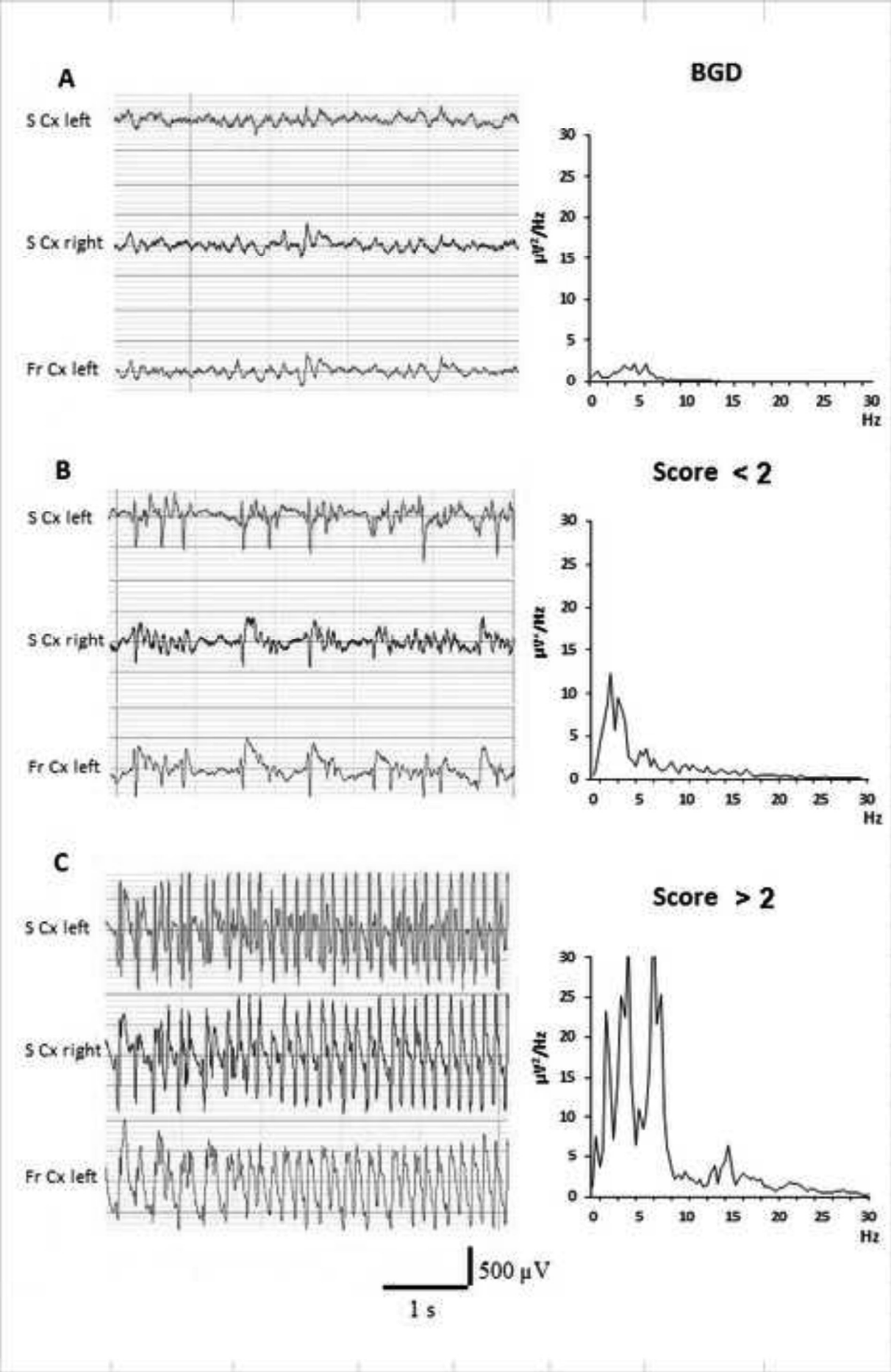


Figure 2
[Click here to download high resolution image](#)

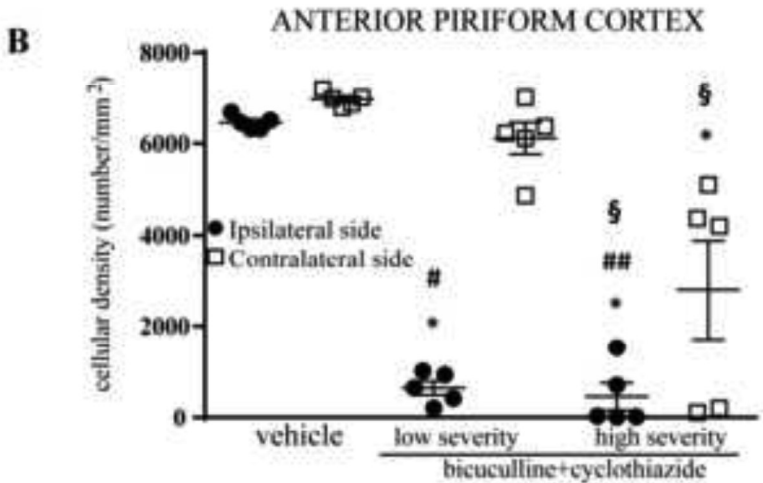
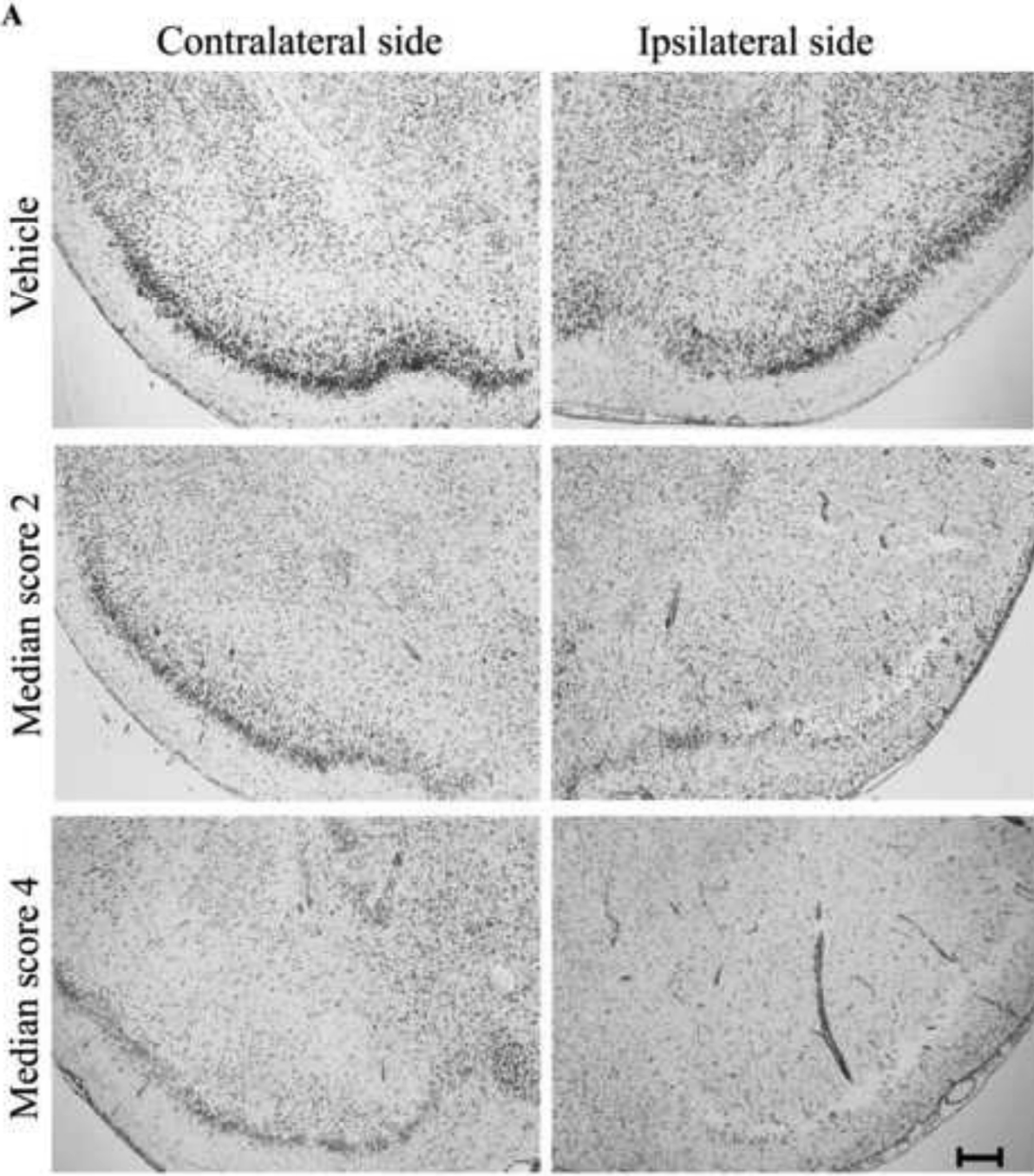


Figure 3
[Click here to download high resolution image](#)

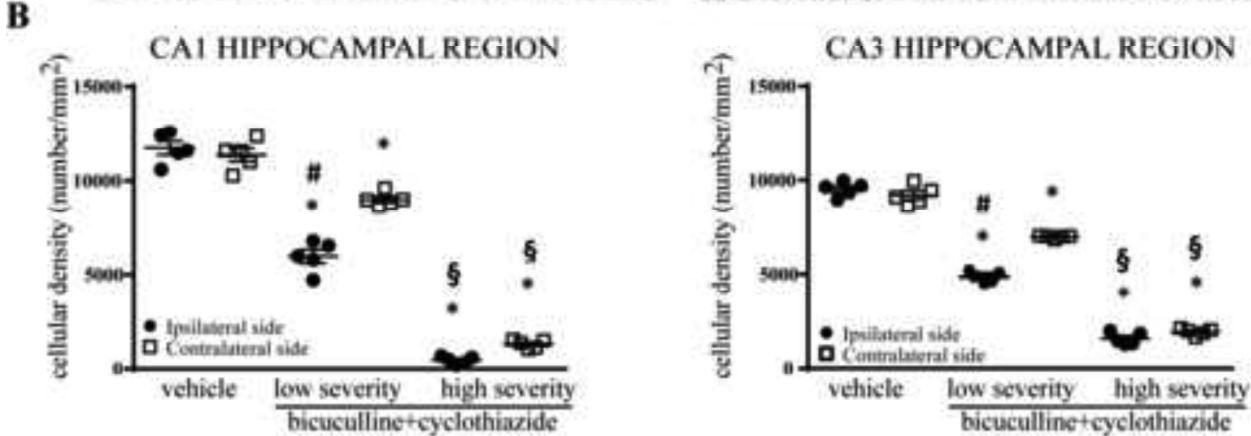
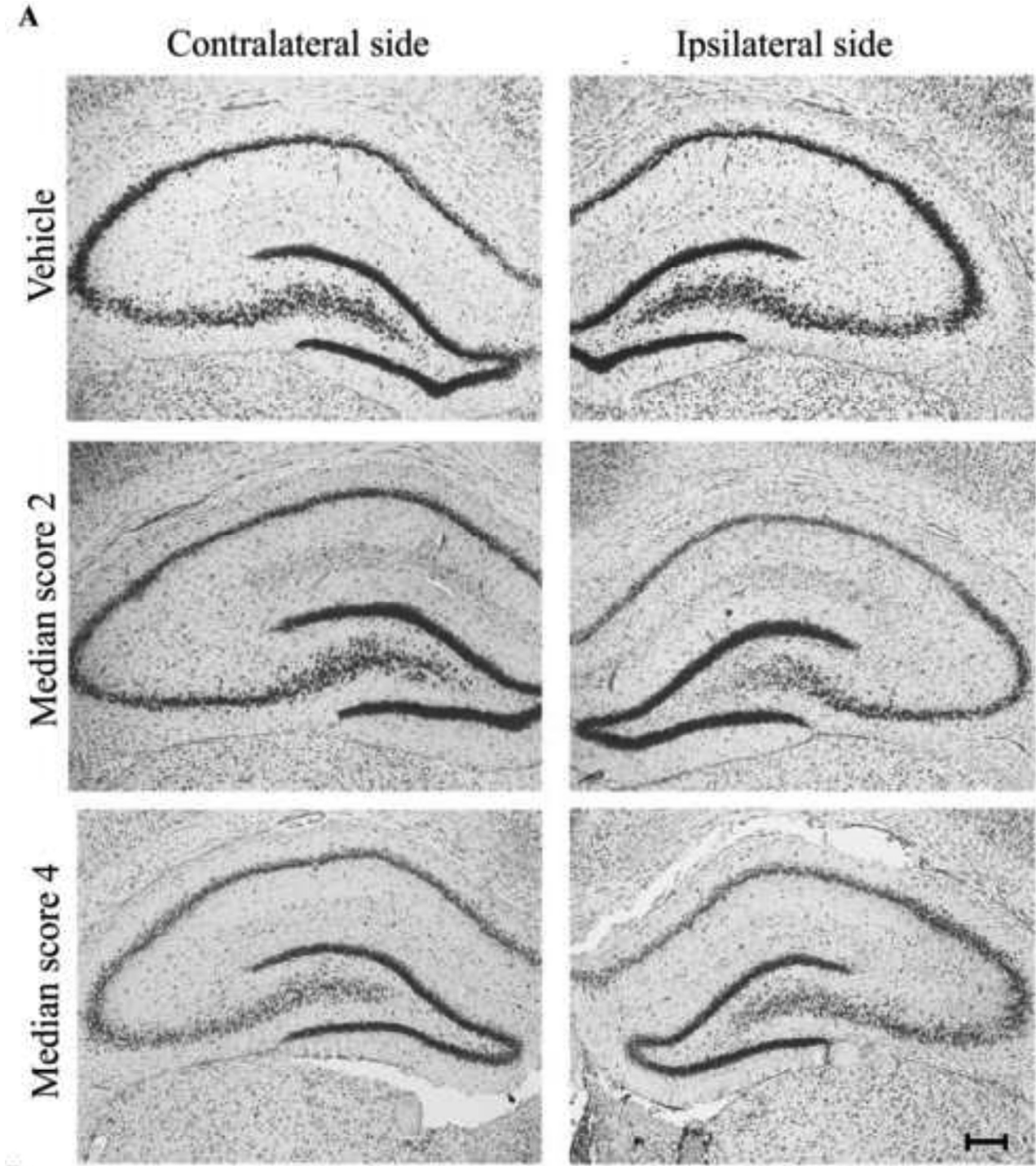


Figure 4
 Click here to download high resolution image

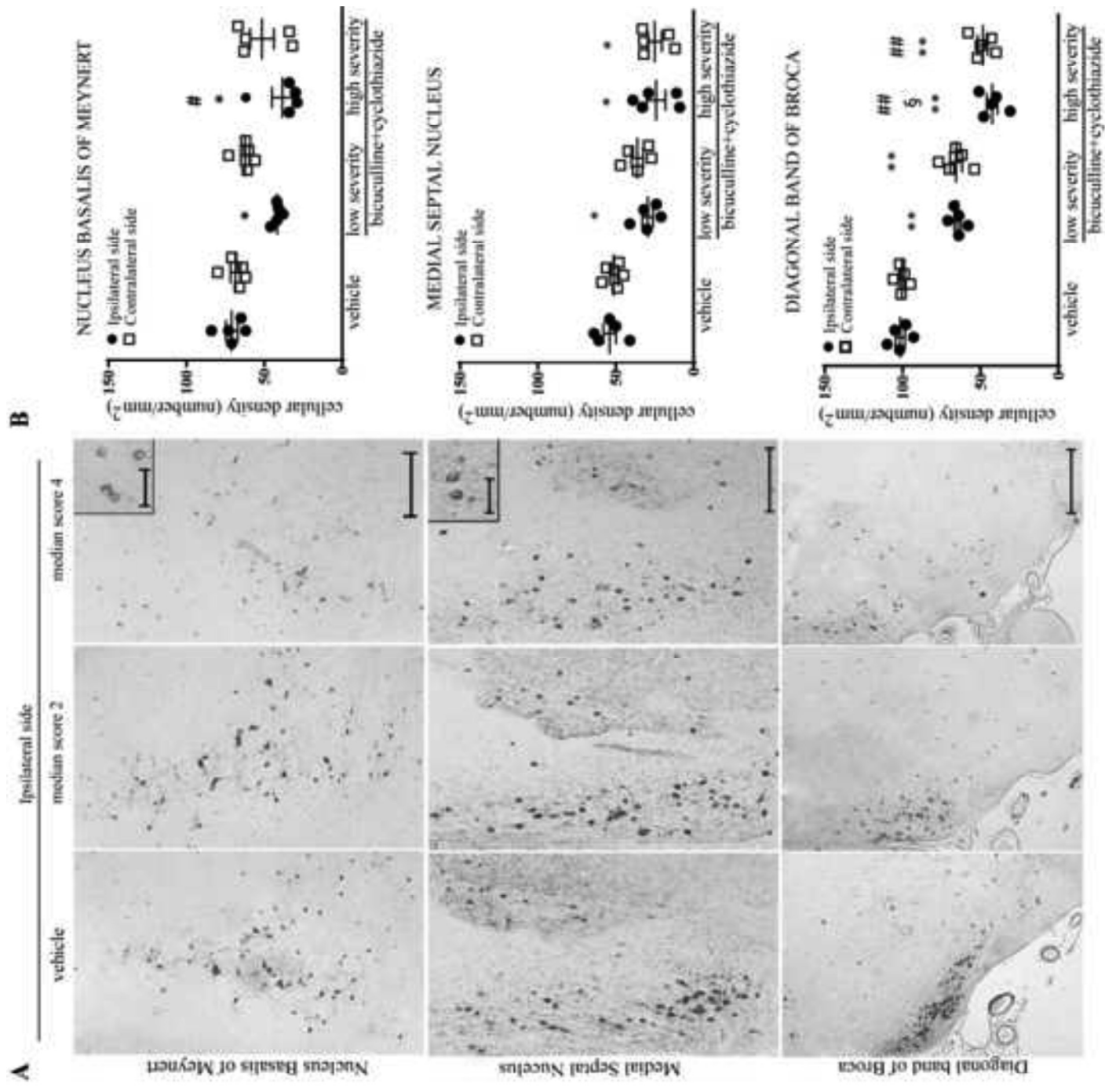


Figure 5
Click here to download high resolution image

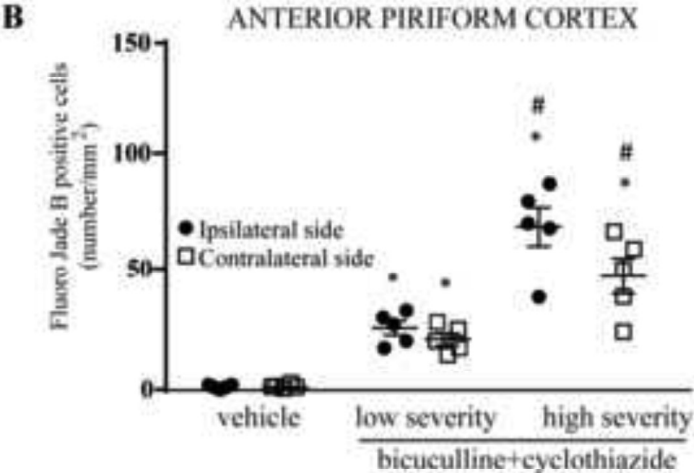
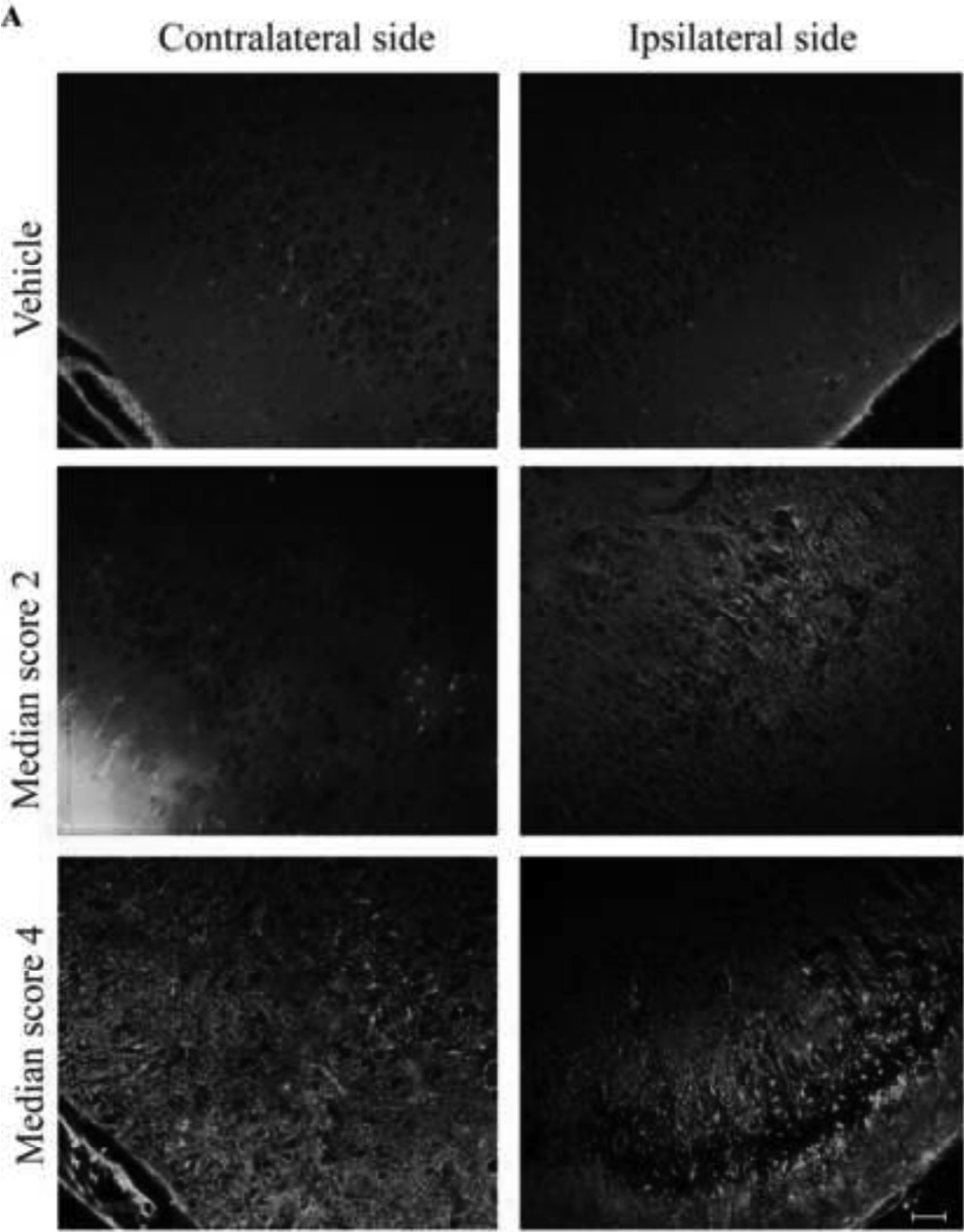


Figure 6
[Click here to download high resolution image](#)

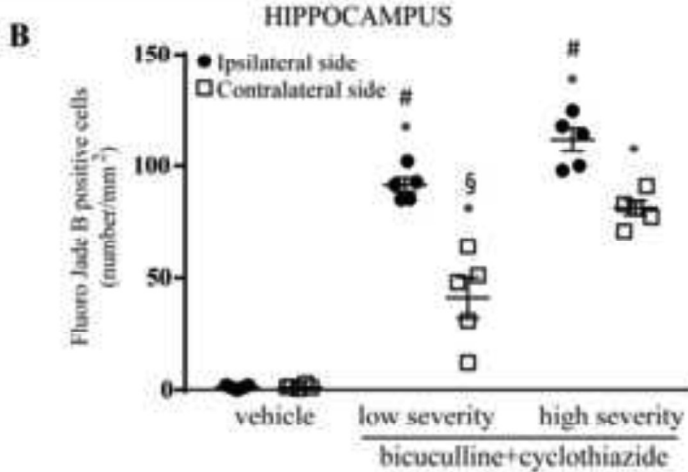
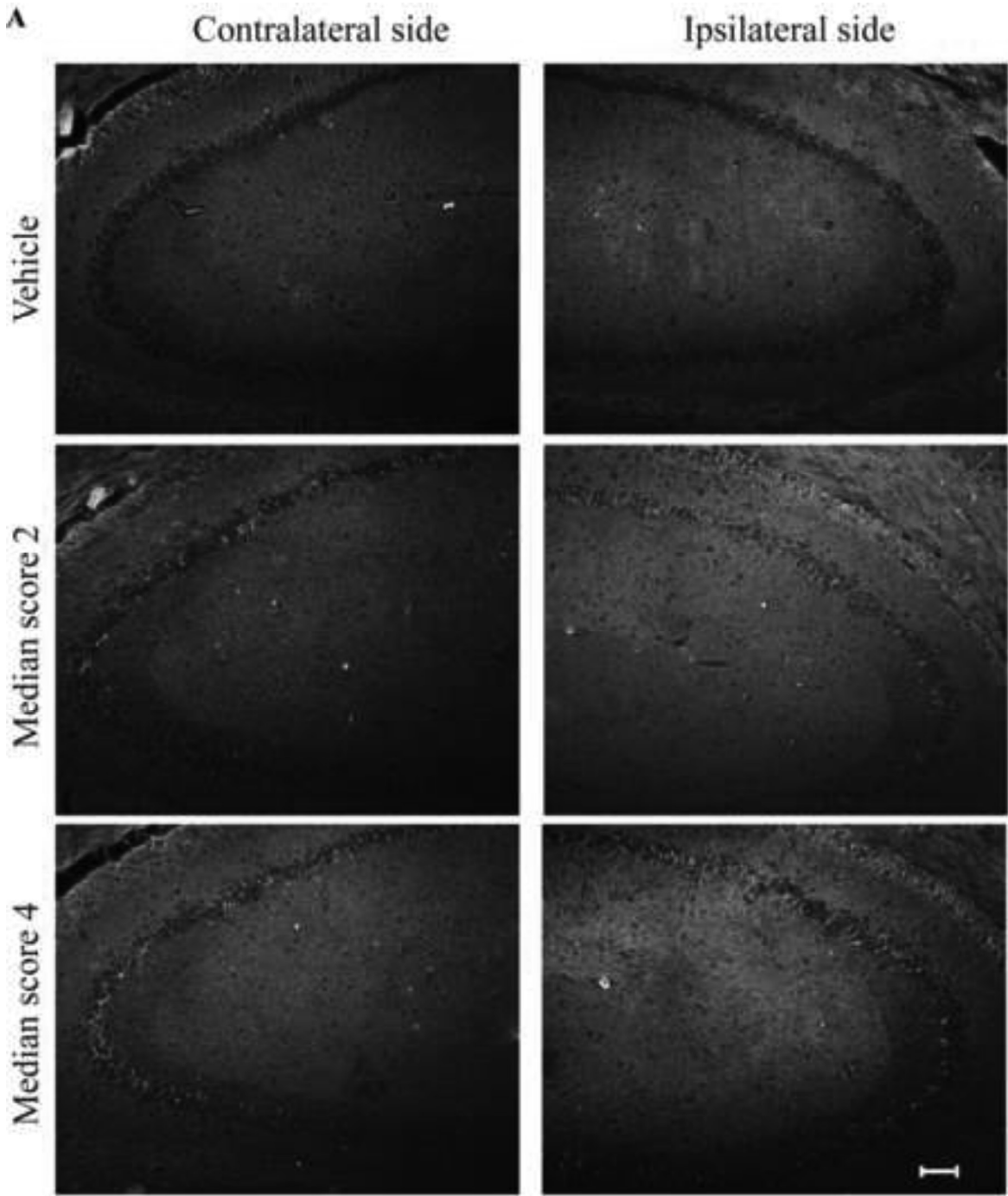


Figure 7
[Click here to download high resolution image](#)

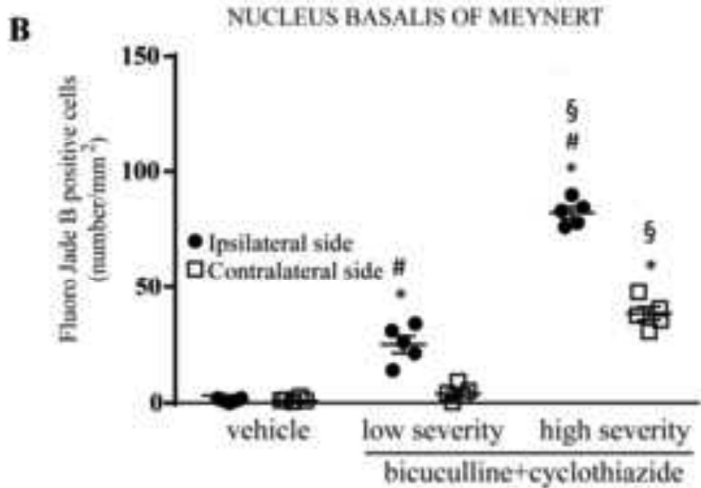
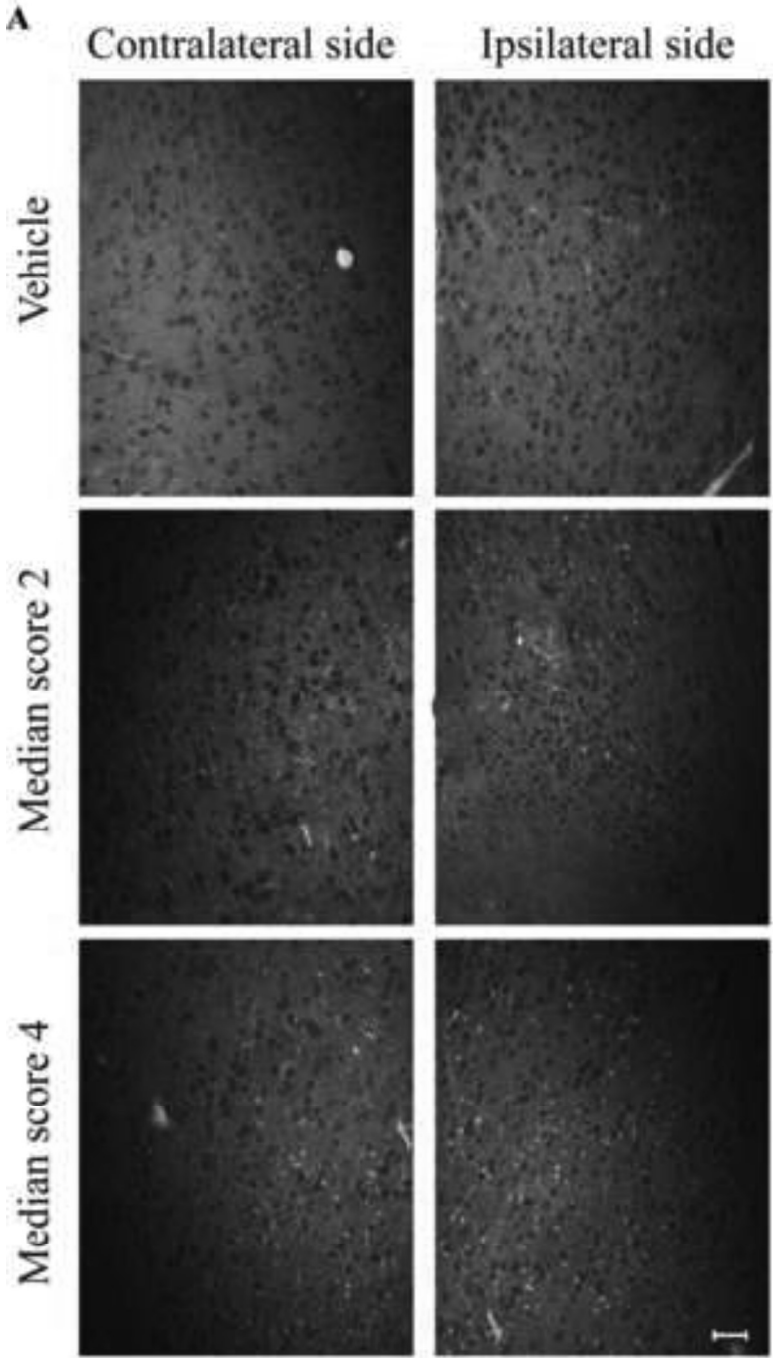


Figure 8
[Click here to download high resolution image](#)

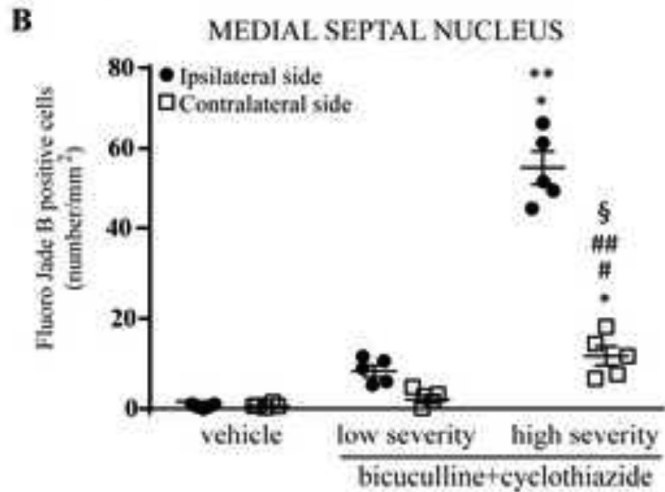
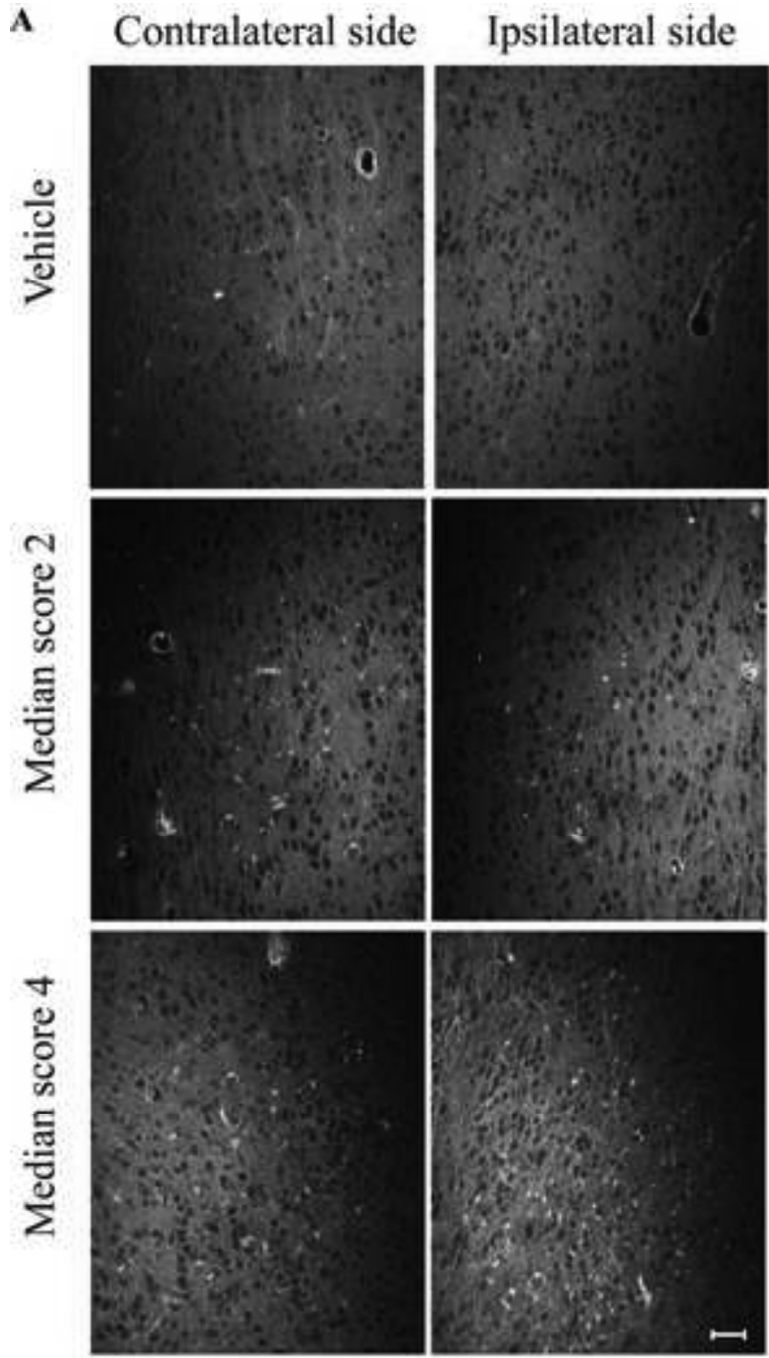


Figure 9
[Click here to download high resolution image](#)

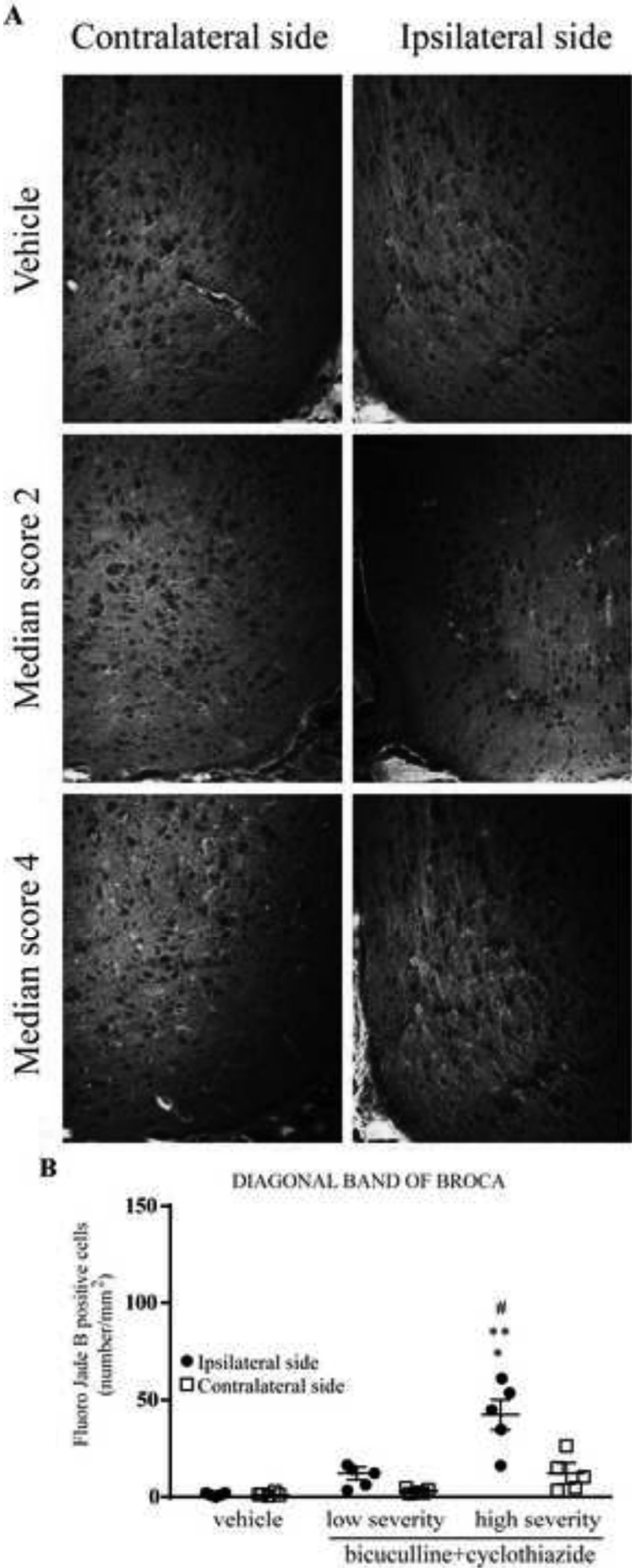


Figure 10
[Click here to download high resolution image](#)

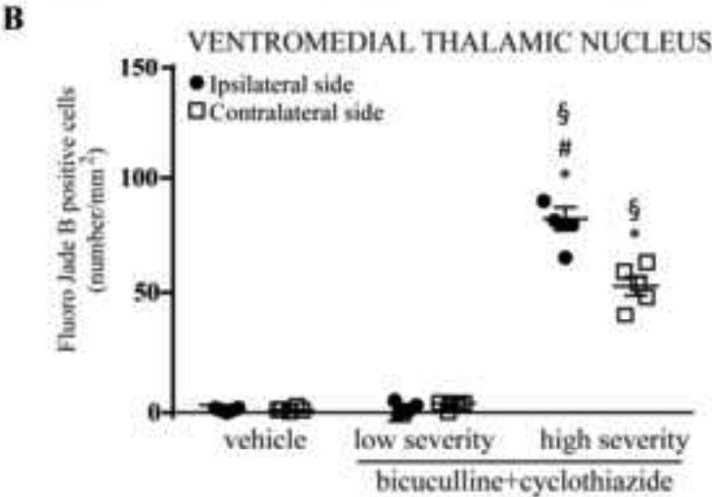
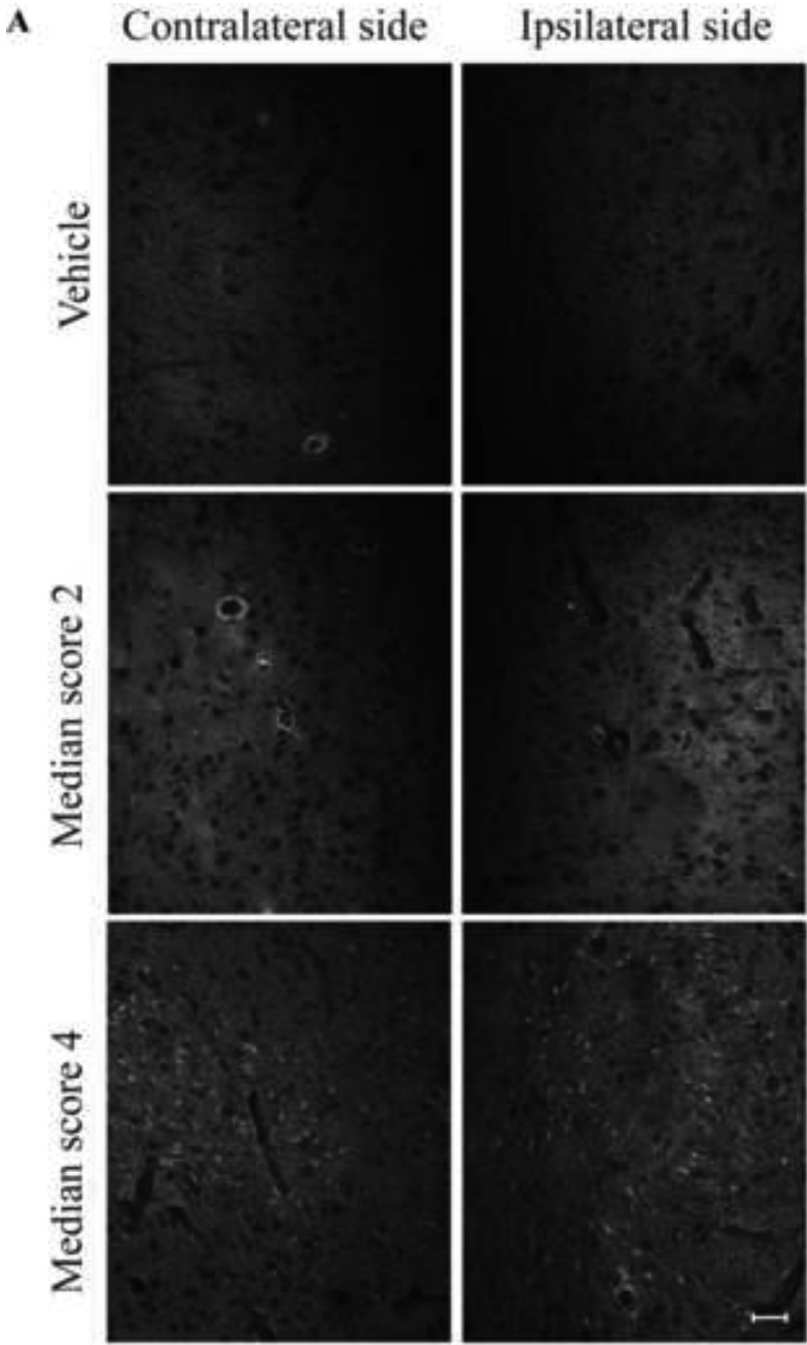


Figure 11
[Click here to download high resolution image](#)

